communications biology

A Nature Portfolio journal

Article

https://doi.org/10.1038/s42003-025-08582-y

Adjuvant activity of a small molecule TLR4 agonist discovered via structure-based virtual screening

Mohammad Kadivella [1,2], Vivek P. Varma [1], Jusail CP [1,2], Sridhar Kavela [1], Sarwar Azam [3] & Syed M. Faisal [1,2]

Monophosphoryl lipid A (MPLA), a TLR4 agonist, is a clinically approved vaccine adjuvant, but its complex structure and occasional toxicity limit broader use. Synthetic small-molecule TLR4 agonists offer advantages such as ease of synthesis, lower cost, and reduced toxicity. In this study, we conducted structure-based virtual screening of the ZINC database to identify novel TLR4-targeting small molecules across human, murine, and bovine species. Three lead compounds—NSF-418, NSF-501, and NSF-951—were selected based on favorable binding interactions and subjected to in vitro and in vivo evaluation. NSF-951 emerged as a potent TLR4 agonist, inducing strong proinflammatory cytokine responses (IL-6, TNF-α), upregulating CD80 and CD86 expression, and promoting macrophage maturation. Conversely, NSF-418 and NSF-501 acted as antagonists by suppressing MPLA-induced responses. In murine immunization studies, NSF-951, alone or with Alum (AF007), significantly enhanced OVA-specific antibody and T-cell responses without observable toxicity. These findings suggest that NSF-951 is a promising, cost-effective TLR4 agonist with strong immunostimulatory and adjuvant potential. Further studies are warranted to assess its performance with other antigens and adjuvant combinations, supporting its development as a next-generation adjuvant for veterinary and human vaccines.

Adjuvants are critical components of vaccines, playing a pivotal role in their efficacy and success[1,2]. Immunostimulatory adjuvants such as MPLA, CpG-ODN, MDP, flagellin, and other TLR agonists enhance antigen-specific immune responses by activating innate immunity[3]. The innate immune system is essential for defending against infections caused by microbial pathogens, recognizing pathogen-associated molecular patterns (PAMPs) like LPS, lipoproteins, flagellin, DNA, and RNA via pattern recognition receptors (PRRs), including Toll-like receptors (TLRs) and Nod-like receptors (NLRs)[4,5]. Certain TLRs, such as TLR1, TLR2, TLR4, TLR5, and TLR6, are expressed on cell surfaces and recognize bacterial cell wall components, while intracellular TLRs like TLR7, TLR8, and TLR9 detect viral RNA and DNA fragments in the endosomal system[6]. TLR activation orchestrates critical immune functions, including immune cell migration, antigen processing, and adaptive immune responses. This activation promotes APC maturation, co-stimulatory molecule expression (e.g., CD80, CD86), and antigen presentation via MHC molecules, ultimately enhancing T cell priming and antibody responses[7].

Among TLRs, TLR4 is the most extensively studied. Located on the plasma membrane, it recognizes lipopolysaccharides (LPS), a key PAMP on Gram-negative bacteria, with the help of co-receptors MD-2 and CD14. TLR4 uniquely activates two signalling pathways via MyD88 and TRIF, leading to NF-κB-mediated pro-inflammatory cytokine production and IRF-induced type I interferon expression, respectively[8–10]. Despite its potency, LPS's high toxicity prevents its use as an adjuvant. Efforts to chemically modify the lipid A region of LPS, which mediates its immunostimulatory activity, have resulted in less toxic derivatives like Monophosphoryl Lipid A (MPLA) and Glucopyranosyl Lipid A (GLA), which retain strong immunopotentiating properties[10,11]. MPLA is already used as a clinical adjuvant in HPV and HBV vaccines in Europe[12,13]. However, MPLA's heterogeneity, high cost, complex synthesis, and dose-dependent toxicity limit its broader application[14].

The discovery of synthetic small-molecule TLR4 agonists mimicking LPS's signalling pathways has significantly advanced vaccinology[15]. These molecules, such as IZ205 and Neoseptin-3, are cost-effective, easy to synthesize, and capable of inducing balanced Th1 and Th2 immune responses,

[1]Laboratory of Vaccine Immunology, National Institute of Animal Biotechnology, Hyderabad, India. [2]Regional Centre for Biotechnology, Faridabad, India. [3]Laboratory of Computational Biology, National Institute of Animal Biotechnology, Hyderabad, India. e-mail: faisal@niab.org.in

enabling antigen dose sparing[16,17]. Traditionally, these agonists were identified through high-throughput screening of chemical libraries, which involved costly and labour-intensive methods. Recent advances in computational chemistry and biology, including computer-aided drug design (CADD), ligand-based virtual screening (LBVS), and structure-based virtual screening (SBVS), have streamlined this process. High-performance computing (HPC) has facilitated the identification of TLR agonists and antagonists with minimal toxicity[18–20]. However, most identified compounds remain restricted to in vitro studies and have not been evaluated for their adjuvant potential in vivo[21].

In this study, we used structure-based virtual screening of natural or economical compounds from the ZINC database to identify small-molecule TLR4-binding candidates. The identified synthetic molecules were commercially procured and assessed for their agonist or adjuvant activity on macrophages derived from mice, humans, and bovines, and their toxicity was assessed in vitro and in vivo. Finally, the identified compounds were tested for their adjuvant efficacy in a mouse model.

Results

Structure-based virtual screening of small-molecule TLR4 binding compounds

The primary objective of this in silico screening was to identify small-molecule compounds capable of binding to TLR4 receptors across different species, including human (hTLR4/MD2), mouse (mTLR4/MD2), and bovine (bTLR4/MD2). Small molecules were docked into the active sites of TLR4-MD2 complexes, and their binding energies were estimated. For these docking studies, receptor flexibility was specifically defined for amino acid residues surrounding the active sites. The parameters for defining the active site (grid box coordinates) of each TLR4-MD2 receptor were provided in Supplementary Table 1. To evaluate ligand binding scores, we assessed the MPLA molecule under identical coordinates using structure-based virtual screening (SBVS). The calculated binding energies of MPLA with hTLR4/MD2, bTLR4/MD2, and mTLR4/MD2 were −6.5 kcal/mol, −5.7 kcal/mol, and −5.7 kcal/mol, respectively (Table 1). Compounds with binding energies close to or better than MPLA were filtered, and the top five hits were further refined to three final candidates: NSF-418 (ZINC96113056), NSF-501 (ZINC96113056) and NSF-951 (ZINC67299692) based on their toxicity profiles and commercial availability or synthesizability (Table 1). Figure 1A illustrates the 2D chemical structures of these three compounds. The binding energies of NSF-951 ranged from −7.7 to −8.5 kcal/mol, while NSF-418 and NSF-501 exhibited ranges of −6.6 to −7.3 kcal/mol and −6.7 to −7.4 kcal/mol, respectively, across different TLR4 receptors (Table 1). The binding poses and interaction patterns of these compounds within the active site of the mTLR4-MD2, hTLR4/MD2 and bTLR4/MD2 complex are shown in (Fig. 1B and Supplementary Fig. 2). Ligplot analysis visualized interactions between mTLR4-MD2 amino acid residues and the compounds, highlighting hydrophobic interactions (red arcs) and hydrogen bonds (green dashed lines) (Fig. 1C). These results indicate that all three compounds interacted similarly with hTLR4 and bTLR4. Despite exhibiting favourable binding interactions with TLR4/MD2 complexes, the compounds displayed varying levels of water solubility. The calculated log *P* values for NSF-418, NSF-501, and NSF-951 were −1.254. −0.334 and 3.645, respectively (Supplementary Table 2), indicating solubility ranging from high to moderate. The RMSD plot illustrates the structural stability of the protein backbone during molecular dynamics simulations. Minimal deviation was observed during the initial period (0–20,000 ps), followed by significant deviations during the middle period (20,000–80,000 ps), and eventual stabilization with minor fluctuations during the final period (80,000–100,000 ps). NSF-418 demonstrated the most stable protein structure with the lowest fluctuations, while NSF-501 exhibited the highest fluctuations. NSF-951 showed intermediate behaviour, suggesting moderate structural stability, slightly less than NSF-418 but more stable than NSF-501 (Fig. 1D). The RMSF plot highlights the flexibility of protein residues during simulations, revealing higher fluctuations at the N-terminus and C-terminus and lower fluctuations in the middle residues. NSF-418 displayed the lowest RMSF values, indicating superior stability, followed by NSF-501 and NSF-951, which showed moderate and higher fluctuations respectively (Fig. 1D). In silico toxicity analysis, performed using Swiss ADME and admetSAR2 (https://lmmd.ecust.edu.cn/admetsar2/), evaluated physicochemical properties and drug-likeness parameters according to Lipinski, Veber, Egan, and Muegge criteria etc (Supplementary Table 2). The small molecules NSF-951, NSF-501, and NSF-418 exhibited favourable ADMET (absorption, distribution, metabolism, excretion, and toxicity) profiles based on admetSAR predictions, indicating their non-mutagenicity (AMES test), non-carcinogenicity, and low acute oral toxicity (Class III). Radar plots demonstrated that all three compounds fell entirely within the pink drug-likeness zone, confirming their non-toxic profiles and favourable ADME properties (Supplementary Fig. 3). All compounds showed low honeybee toxicity, minimal renal transporter inhibition, and lysosomal localisation, characteristics associated with endosomal TLR targeting. NSF-501 displayed moderate blood-brain barrier permeability, while NSF-951 and NSF-418 are non-permeable, reducing CNS off-target effects. Minimal CYP450 and hERG inhibition suggest low risks of drug-drug interactions and cardiotoxicity. To understand the mechanism and residues involved in binding, in silico mutagenesis was conducted on critical residues inside the mTLR4-MD2 (PDB ID: 3T6Q) binding pocket utilising PyMOL's mutagenesis wizard to investigate their role in NSF-951 binding. The wild-type mTLR4-MD2 (PDB ID: 3T6Q) had a binding energy of –8.5 kcal/mol, establishing the baseline. Within the mutants, Y122A and I68V in Chain C exhibited increased binding affinities of –9.6 and –9.9 kcal/mol, respectively, indicating higher ligand accommodation. In contrast, mutations like L101A (–7.8 kcal/mol) and L142A (–7.4 kcal/mol) resulted in diminished binding, suggesting impaired hydrophobic or structural interactions (Supplementary Table 3).

Screening of selected compounds for immunomodulatory activity in macrophages from different host species

Synthetic NSF-418, NSF-501, and NSF-951 were purchased from Molport, USA. The toxicity of these compounds was initially assessed on mouse

Table 1 | TLR4-MD2 binding energy, toxicity and synthesizability of small molecules identified from the ZINC database through Structure-Based Virtual Screening

Compound Name	ZINC ID	Binding energy (kcal/mol) with TLR4-MD2			Toxicity	Synthesisability
		Mouse	Bovine	Human		
MPLA	Not Applicable	−5.7	−5.7	−6.5	NO	✓
NSF-418	ZINC20465113	−7.3	−6.6	−6.9	NO	✓
NSF-501	ZINC96113056	−7.4	−6.7	−6.8	NO	✓
NSF-534	ZINC106803392	−6.6	−7.3	−6.7	YES	✓
NSF-856	ZINC95914806	−6.7	−7.3	−6.9	YES	×
NSF-951	ZINC67299692	−8.5	−7.9	−7.7	NO	✓

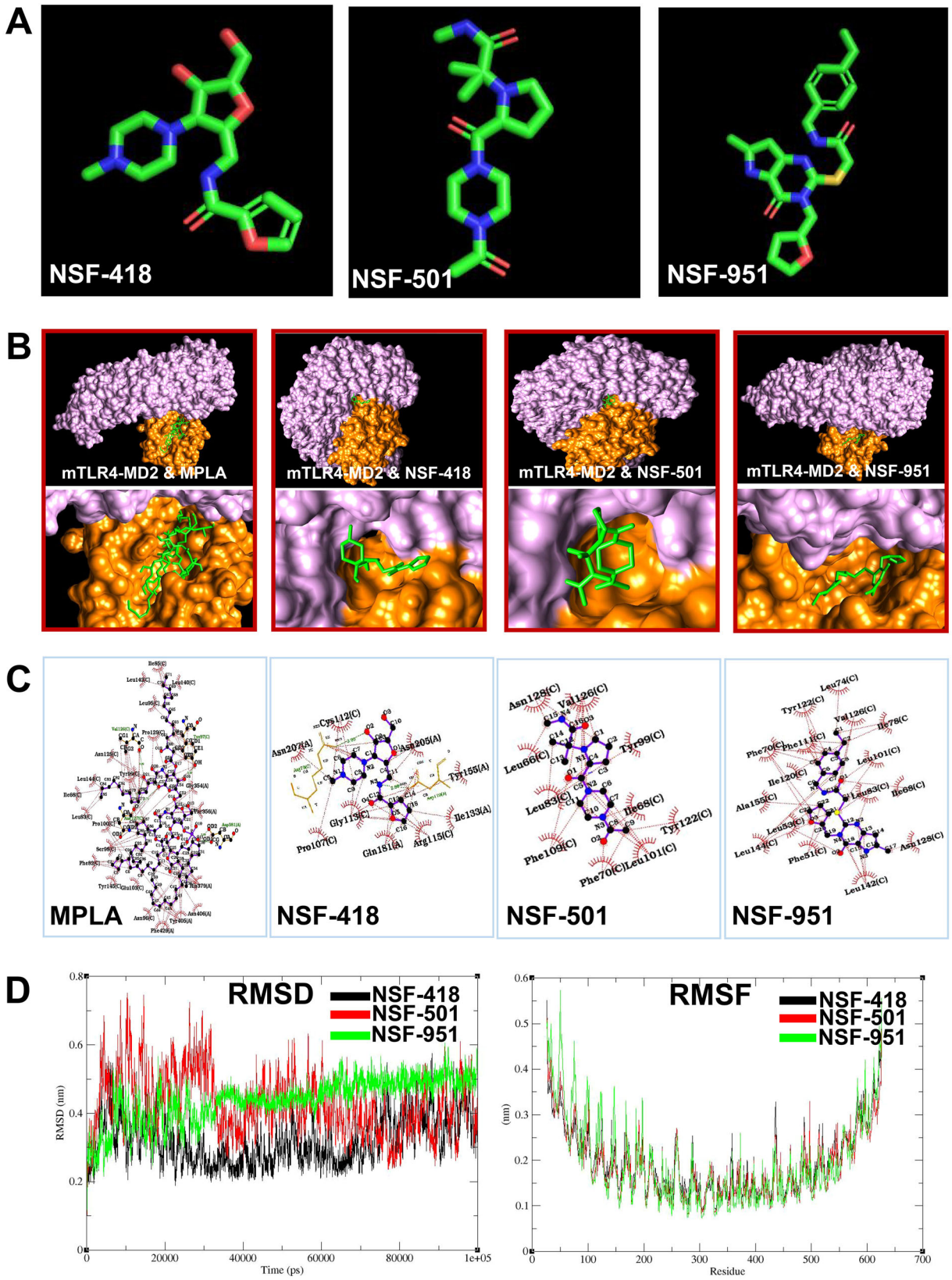

Fig. 1 | In silico analysis of TLR4 binding compounds. A The 2D structures of small molecule TLR4-binding compounds were visualised in PDB format using PyMOL Green indicates carbon (C), Red indicates oxygen (O), yellow-sulphur(S), and blue indicates Nitrogen. **B** Molecular docking of the compounds with mouse TLR4-MD2 receptors. The small molecule compounds (green) as well as MPLA (green) were docked at the active sites of the mouse TLR4-MD2 which includes LRR domain (shown in pink) and MD2 (shown in orange). **C** Ligplot analysis illustrating the interactions between the compounds and mouse TLR4-MD2 complex. Hydrophobic interactions are represented by red arcs, while hydrogen bonds are depicted as green dashed lines with bond lengths specified. **D** Molecular dynamics simulation analysis of compounds-mTLR4 complexes. A Root Mean Square Deviation (RMSD) of the protein backbone, indicating the stability of the protein-ligand complexes over simulation time b) Root Mean Square Fluctuation (RMSF), showing the flexibility of individual amino acid residues in the mTLR4 protein for each compound-TLR4 complex.

macrophages using the MTT assay. Our results showed that none of the compounds (NSF-418, NSF-501, NSF-951) exhibited significant toxicity at concentrations up to 200 μM (Supplementary Fig. 4). To evaluate their potential to activate mouse macrophages, RAW 264.7 cells were stimulated with varying concentrations of NSF-418, NSF-501, or NSF-951 (0.2 μM-20 μM), and the production of pro-inflammatory cytokines IL-6 and TNF-α were analyzed. Macrophages stimulated with MPLA (2 μg/mL) served as the control. Among the three TLR4-binding compounds, only NSF-951 induced significant, dose-dependent levels of IL-6 and TNF-α. To assess the functional potency of NSF-951, the resulting TLR4-mediated response (IL-6) was quantified. A sigmoidal dose–response curve was obtained. The analysis yielded an EC_{50} value of 253.4 nM, indicating the concentration at which NSF-951 induces half-maximal activation under the tested conditions. This value reflects a moderate functional potency consistent with effective TLR4 pathway engagement. whereas NSF-418 and NSF-501 did not induce appreciable levels of these cytokines (Fig. 2A, Supplementary Figs. 5 and 6A). The expression of co-stimulatory molecules (CD80, CD86) and the maturation marker (MHC-II) on macrophages activated by these compounds was analyzed via flow cytometry. NSF-951 significantly upregulated the expression of these molecules to levels comparable to MPLA, while NSF-418 and NSF-501 failed to do so (Fig. 2A, B and Supplementary Fig. 7). To further investigate innate immune modulation, the expression of other innate immune genes, including cytokines, chemokines, and their receptors, was analyzed in macrophages stimulated with these compounds using qRT-PCR. NSF-951 uniquely modulated the expression of chemokines (CCL2, CCL5, CCL8, CXCL10), cytokines (IL-6, TNF-α, IL-1β), and other inflammatory mediators such as iNOS, COX-2, MIP1α, and MCP1. In contrast, NSF-418 and NSF-501 failed to induce significant modulation of these genes (Fig. 2A, C). Given the ability of these compounds to bind TLR4 receptors in humans and bovines, we tested their activity on macrophages derived from these species. Of the three TLR4-binding compounds, only NSF-951 significantly induced the production of pro-inflammatory cytokines and modulated the expression of several cytokine and chemokine genes in both human and bovine macrophages (Fig. 2B, C and Supplementary Fig. 6B, C). To evaluate whether NSF-951 could activate primary immune cells, we stimulated mouse bone marrow-derived dendritic cells (BMDCs) and bovine peripheral blood mononuclear cells (PBMCs) with NSF-951. The compound significantly induced pro-inflammatory cytokine production in both cell types (Supplementary Fig. 8). Taken together, these findings demonstrate that NSF-951 is a potent immunostimulatory molecule capable of activating innate immune cells across multiple host species.

NSF-951 is a TLR4 agonist whereas NSF-418 and NSF-501 demonstrated antagonist activity

To determine whether the response induced by NSF-951 is mediated through the TLR4 receptor, we stimulated murine wild-type (WT) and $TLR4^{-/-}$ macrophages with NSF-951, NSF-418, or NSF-501 and analyzed the production of pro-inflammatory cytokines. WT macrophages produced significant levels of IL-6 and TNF-α upon stimulation with NSF-951, whereas $TLR4^{-/-}$ macrophages failed to produce these cytokines, confirming that NSF-951 acts as a TLR4 agonist (Fig. 3A). Given that NSF-418 and NSF-501 bind to TLR4 but do not induce a pro-inflammatory response in macrophages from various species, we hypothesized that these compounds might act as TLR4 antagonists. To test this, RAW264.7 cells were pre-treated with NSF-418 or NSF-501, followed by stimulation with MPLA, and the production of pro-inflammatory cytokines was analyzed. Both NSF-418 and NSF-501 inhibited MPLA-induced cytokine production, confirming their roles as TLR4 antagonists (Fig. 3B). To evaluate whether NSF-418, NSF-501, and NSF-951 directly bind to the leucine-rich repeat (LRR) domain of TLR4 in the absence of MD-2, we performed microscale thermophoresis (MST) assays using recombinant mouse TLR4 ectodomain protein. The binding profiles were generated by titrating each compound across a concentration range of 500 μM to 0.244 μM, and the resulting thermophoretic shifts were analyzed to determine equilibrium dissociation constants K_D Among the tested ligands, NSF-951 exhibited the strongest binding affinity with a K_D of 16.01 μM (±33.24 μM), followed by NSF-418 with a K_D of 213.17 μM (±830.00 μM), and NSF-501 with a K_D of 1462.20 μM (±2174.40 μM). MPLA, the reference TLR4 agonist, displayed a K_D of 575.42 μM (±1057.40 μM). Despite large confidence intervals, the data indicate that NSF-951 has comparatively stronger direct binding to TLR4 under these conditions. However, the moderate-to-high error margins, particularly for MPLA and NSF-501, suggest that binding in the absence of MD-2 may be weak, unstable, or conformationally dynamic (Supplementary Fig. 9).

NSF-951 activates macrophages via MyD88 using P38 and JNK pathways

To investigate whether NSF-951 induces signalling through membrane activation involving the TIRAP-MyD88 adapter or endocytosis involving the TRAM-TRIF adapter, we stimulated $MyD88^{-/-}$ and $TRIF^{-/-}$ macrophages with NSF-951 and analysed cytokine production. $TRIF^{-/-}$ macrophages produced significant levels of cytokines upon stimulation, whereas cytokine levels were significantly reduced in $MyD88^{-/-}$ macrophages, indicating that NSF-951 signals primarily through the MyD88 adapter (Fig. 4A). To explore potential involvement of TRIF-TRAM-dependent signalling, we stimulated WT and $TRIF^{-/-}$ macrophages with NSF-951 and analysed the expression of IFN-related cytokines (MCP-1, IP-10, IFN-β, and RANTES) at 24 hrs via qRT-PCR. NSF-951 significantly upregulated the expression of these cytokines suggesting some TRIF-TRAM pathway involvement (Fig. 4B). The role of the MAP kinase pathway in NSF-951-induced signalling and cytokine production was further investigated by analyzing the phosphorylation of p38, JNK, and ERK via western blot. NSF-951 induced strong phosphorylation of p38 and JNK, similar to MPLA (Fig. 4C and Supplementary Fig. 10). To confirm the functional relevance of these kinases, RAW264.7 cells were pre-treated with pharmacological inhibitors of NF-κB, JNK, p38, or ERK, followed by stimulation with NSF-951. Inhibition of p38, JNK, or NF-κB significantly blocked IL-6 and TNF-α production ($P < 0.05$), while ERK inhibition had no effect, indicating that ERK is not involved in NSF-951-induced signalling (Fig. 4D). These findings collectively demonstrate that NSF-951 primarily signals through the MyD88 adapter and activates macrophages by inducing pro-inflammatory cytokines via the p38, JNK, and NF-κB pathways.

Evaluation of in vivo adjuvant activity of NSF-951

MPLA is known to enhance antigen-specific immune responses. Given that NSF-951 induced a strong innate immune response comparable to MPLA (as evidenced by significant macrophage activation), we tested its ability to enhance antigen-specific immune responses. Mice were immunized with a model antigen, ovalbumin (OVA), formulated with or without MPLA or NSF-951 or NSF-418 or NSF-501. Animals were subsequently boosted with the same formulations, and OVA-specific antibody levels were analyzed in serum via ELISA. The results revealed significantly higher levels of IgG on day 28 in the OVA + MPLA and OVA + NSF-951 groups compared to OVA alone, indicating that NSF-951 mediates an adjuvant effect by enhancing antigen-specific antibody responses (Fig. 5A). Additionally, lymphocytes isolated from mice immunized with OVA + NSF-951 secreted significantly higher levels of both Th2 (IL-4) and Th1 (IFN-γ) cytokines compared to those from the OVA-only group (Fig. 5B, C). As expected, neither NSF-418 nor NSF-501 enhanced OVA-specific antibody or T-cell responses, and their effects were similar to those observed in animals immunized with OVA alone (Fig. 5A–C). These findings confirm the in vivo adjuvant activity of NSF-951. Since MPLA is known to enhance the potency of Alum in AS04, we also tested whether NSF-951 could act as a co-adjuvant to amplify the efficacy of Alum. A formulation combining NSF-951 and Alum, referred to as Adjuvant Formulation 007 (AF007), was developed (Fig. 5D). Mice were immunized with PBS or OVA formulated in Alum or AS04 or AF007, and then boosted. OVA-specific antibody and T-cell responses were subsequently analyzed. Our results showed that NSF-951 in AF007 acted as a strong co-adjuvant, amplifying the adjuvant effect of

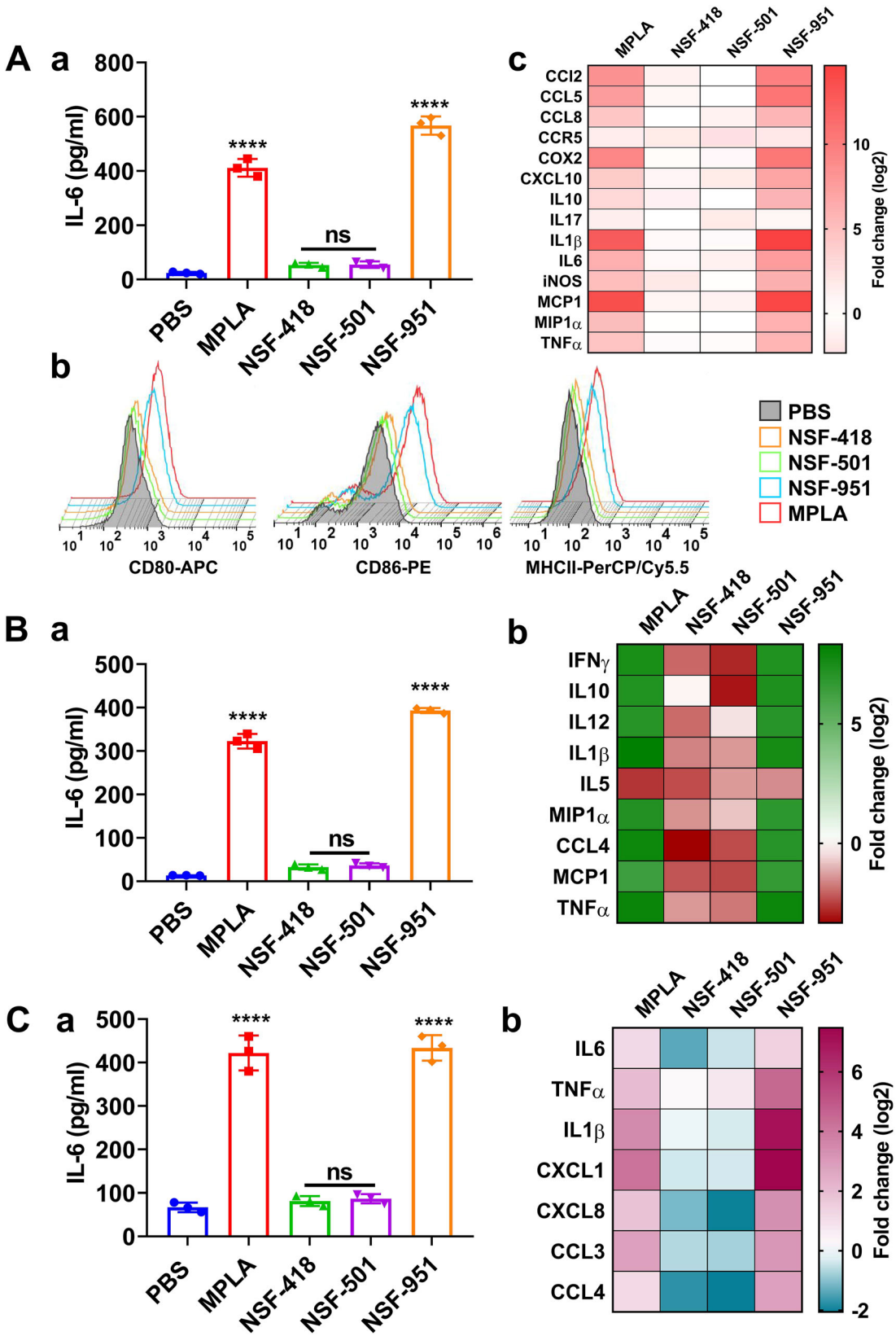

Alum. The OVA-AF007 group generated significantly higher antibody levels compared to the OVA-Alum group (Fig. 5E). OVA-AF007 induced elevated levels of both IgG1 (Th2) and IgG2c (Th1), similar to MPLA (Fig. 5F). Cytokine analysis revealed that while AF007 enhanced IL-4 levels, it induced significantly higher IFN-γ levels, indicating a Th1-skewed response (Fig. 5G, H). Interestingly, the immune responses induced by the AF007 formulation were similar to those generated by AS04. Overall, these findings demonstrate that NSF-951 is a potent adjuvant capable of enhancing antigen-specific immune responses both alone and in combination with Alum.

Fig. 2 | Adjuvant activity of TLR4 binding compounds in vitro. **A** *Proinflammatory/innate activity of compounds in mouse macrophages*. (a) RAW 264.7 cells were treated with 2 μg/mL MPLA (1.13 μM), or 2 μM of NSF-418 (0.679 μg/mL) or NSF-501(0.649 μg/mL) or NSF-951 (0.873 μg/mL) for 24hrs at 37 °C/ 5%CO_2 and production of proinflammatory cytokine (IL-6) was analysed in the culture supernatant by sandwich ELISA as described in methodology. (b) RAW 264.7 cells treated as above were harvested and stained with fluorochrome-conjugated anti-CD80, anti-CD86, and anti-MHCII and expression of the markers was analysed by flow cytometry. (c) RAW 264.7 cells treated as above were harvested, total RNA was isolated, converted to cDNA and modulation of select genes was analysed by qRT-PCR as described in the materials and methods. **B** *Proinflammatory/innate activity of compounds in Human macrophages*. (a) PMA-treated THP-1 monocytes (macrophages) were stimulated with the compounds as described above and production of IL-6 was analysed in the culture supernatant by sandwich ELISA as described in methodology. (b) THP-1 macrophages stimulated as above were harvested, total RNA was isolated, converted to cDNA and modulation of select genes was analysed by qRT-PCR as described in the Materials and Methods. **C** *Proinflammatory/innate activity of compounds in Bovine macrophages*. (a) Bovine macrophages (BoMac cells) were stimulated with the compounds as described above and production of IL-6 was analysed in the culture supernatant by sandwich ELISA as described in methodology. (b) BoMac cells stimulated as above were harvested, total RNA was isolated, converted to cDNA and modulation of select genes was analysed by qRT-PCR as described in the material and methods. The data were presented as fold changes between stimulated cells vs. control and normalized to GAPDH. All data represent the mean ± SD of triplicates ($n = 3$) and are representative of three independent biological experiments. Significant differences were analyzed using one-way analysis of variance (ANOVA), followed by the Dunnett post hoc test. The value of $p < 0.05$ was considered statistically significant and noted as $^{****}p < 0.0001$ and "ns" as not significant.

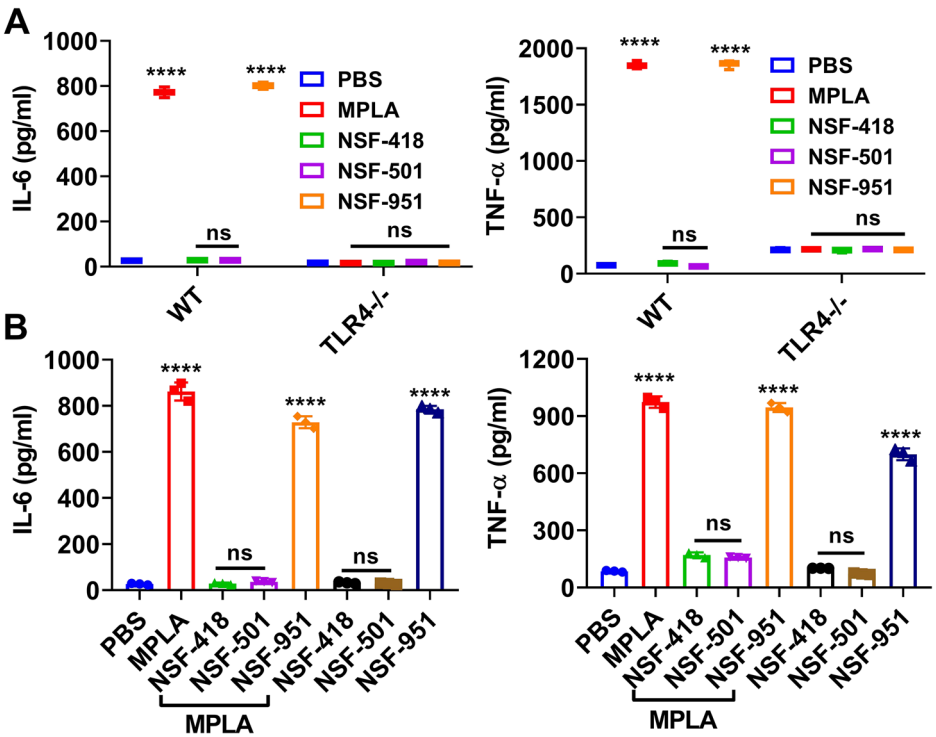

Fig. 3 | TLR4 agonist and antagonist activity of the compounds. **A** *TLR4 agonist activity of compounds*. WT and $TLR4^{-/-}$ mouse macrophage cell lines were stimulated with 2 μg/mL MPLA (1.13 μM), or 2 μM of NSF-418 (0.679 μg/mL) or NSF-501(0.649 μg/mL) or NSF-951 (0.873 μg/mL) for 24hrs at 37 °C/5%CO_2 and production of proinflammatory cytokines (IL-6 and TNF-α) was analysed in the culture supernatant by sandwich ELISA as described in methodology. **B** *TLR4 antagonist activity of compounds*. RAW 264.7 cells were treated with the compounds as described above, followed by treatment with MPLA (2 μg/mL) for 24 hrs at 37 °C/ 5%CO_2 and production of proinflammatory cytokines (IL-6 and TNF-α) was analysed in the culture supernatant by sandwich ELISA as described in methodology. All data represent the mean ± SD of triplicates ($n = 3$) and are representative of three independent biological experiments. Significant differences were analysed using one-way analysis of variance (ANOVA), followed by the Dunnett post hoc test. The value of $p < 0.05$ was considered statistically significant and noted as $^{****}p < 0.0001$ and "ns" as not significant.

Assessment of the toxicity of NSF-951

Before evaluating the in vivo toxicity of NSF-951, it was tested in vitro in additional cell lines of different species such as Human and Bovine macrophages to provide a more comprehensive evaluation of its toxicity profile and potential off-target effects. Our result indicates that NSF-951 did not show any significant level of toxicity up to 200 μM in both THP-1 and BoMac cell lines (Fig. 6A). The in vivo toxicity of NSF-951 was evaluated in mice under both acute and chronic conditions. Our results indicate that NSF-951 did not induce significant toxicity, as evidenced by the absence of notable changes in body weight or temperature at various time points (Fig. 6B, C). Histopathological analysis of vital organs, including the kidneys, liver, lungs, heart, spleen, and brain, showed no significant toxicity even at higher single or repeated doses of 2 mg/kg. Furthermore, NSF-951 combined with Alum (AF007) demonstrated no significant toxicity (Fig. 6D). Accumulation of glial cells in the brain was observed in the animals treated with a low dose (0.5 mg/kg) indicating a mild neuroimmune response (Fig. 6D). However, higher doses or repeated administration did not exacerbate this response, indicating a threshold effect. Normal renal morphology across all treatment groups suggested that NSF-951, either alone or in combination with Alum, did not induce significant changes in kidney structure or function, reflecting its renal safety (Fig. 6D). Mild liver pigmentation observed in the low-dose group (0.5 mg/kg) whereas at higher doses (2 mg/kg), severe liver changes, including multifocal necrosis and inflammation, were observed, indicating dose-dependent hepatotoxicity (Supplementary Fig. 11A, B). Interestingly, animals treated with very high doses (5 mg/kg) or repeated doses (2 mg/kg) showed no significant liver damage, suggesting the possibility of an adaptive response or a threshold effect (Fig. 6D). No abnormalities were observed in the lungs across all treatment groups, supporting the respiratory safety of NSF-951. Mild spleen pigmentation in the low-dose group (0.5 mg/kg) suggested a mild inflammatory response or alterations in iron metabolism, consistent with NSF-951's adjuvant properties. Additionally, mild hypertrophy of lymphatic follicles at higher doses (2 mg/kg and 5 mg/kg) suggested an immunostimulatory effect, contributing to the enhanced immune response (Supplementary Fig. 11C, D). In summary, NSF-951 demonstrated a favourable safety profile at therapeutic doses, with minimal toxicity and potential dose-dependent effects that warrant further investigation.

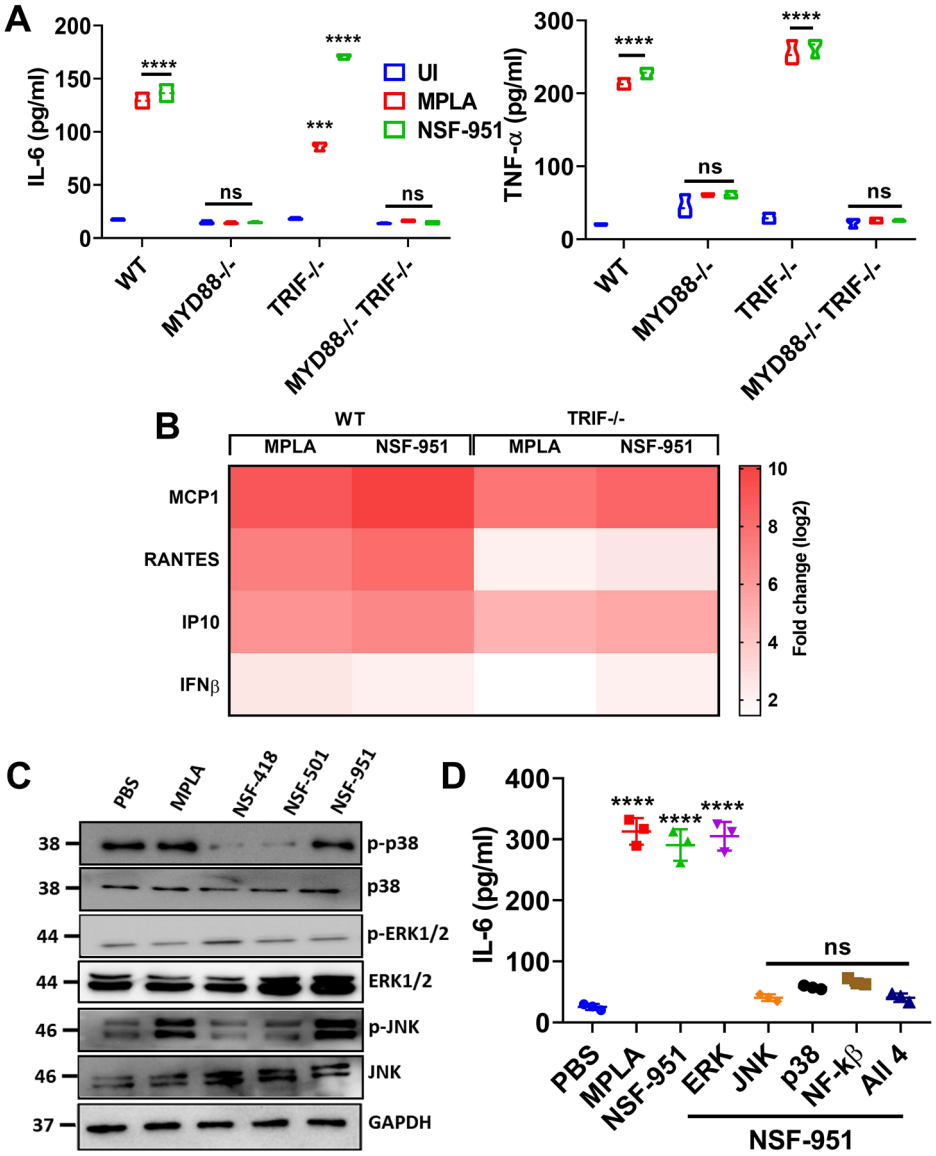

Fig. 4 | NSF-951 induces the pro-inflammatory cytokines via MyD88/TRIF signalling through p38 and JNK-dependent MAPK pathway. **A** Analysis of adapter molecule involved in signalling through NSF-951. WT, MyD88$^{-/-}$, TRIF$^{-/-}$ and TRIF$^{-/-}$/MyD88$^{-/-}$ mouse macrophage cell lines were treated with MPLA (2 μg/mL) or NSF-951 (2 μM) for 24 h at 37 °C in the presence of 5%CO2 and levels of IL-6 and TNF-α were measured in culture supernatant using a sandwich ELISA kit. **B** qRT-PCR analysis of TRIF signalling-associated cytokines and chemokines in NSF-951 stimulated macrophages. WT and TRIF$^{-/-}$ cells were stimulated with MPLA (2 μg/mL) or NSF-951 (2 μM) for 24 hrs at 37 °C/5%CO_2. Cells were recovered and RNA was isolated and converted to cDNA and IFN-1 pathway gene expression was analysed by qRT-PCR as described in the Materials and Methods. **C** Western blot analysis of phosphorylation of mediators of MAP kinase pathway in macrophages stimulated with NSF-951. RAW264.7 cells were stimulated with MPLA (2 μg/mL) or 2 μM of NSF-418 or NSF-501 or NSF-951 for 24 h at 37 °C in 5% CO2. Levels of p38, JNK, and ERK1/2 and respective phosphorylated forms were analysed by western blot as described in materials and methods. **D** *Analysis of MAP kinase signalling pathway in mouse macrophages stimulated with NSF-951.* RAW264.7 cells pre-treated with pharmacological inhibitors of NF-kB (SN50; 20 μM), JNK (SP600125; 40 μM) or p38 (SB203580; 30 μM) or ERK (U0126; 50 μM) or combined together (All 4) for 30 min and then stimulated with MPLA (2 μg/mL) or NSF-951 (2 μM) for 24 h at 37 °C in the presence of 5%CO_2 and supernatant was collected to measure levels of IL-6 by ELISA. All data represent the mean ± SD of triplicates ($n = 3$) and are representative of three independent biological experiments. Significant differences were analysed using one-way analysis of variance (ANOVA), followed by the Dunnett post hoc test. The value of $p < 0.05$ was considered statistically significant and noted as ***$p < 0.001$, ****$p < 0.0001$ and "ns" as not significant.

Discussion

The significance of TLR activation to induce innate and subsequent antigen-specific adaptive immune response can be realized by the fact that several successful live attenuated vaccines, including BCG and Yellow Fever (YF-17D) induce innate immunity by activating multiple TLRs[22,23]. Additionally, some inactivated vaccines, such as influenza vaccines, activate the innate immune system via TLR7 and MyD88-dependent signalling pathways[24]. These insights have driven the rational design of TLR agonists as critical components in developing potent adjuvant formulations. Numerous studies have demonstrated the efficacy of synthetic TLR ligands in enhancing antigen-specific immune responses in mice and non-human primates[25,26]. Several second-generation adjuvants containing TLR agonists have been developed, including AS01 (MPLA + QS21) and AS04 (MPLA + Alum), which are incorporated in vaccines like herpes, hepatitis B (Fendrix), and human papillomavirus vaccines. In these formulations, the TLR4 agonist MPLA serves as an essential component[15,27,28]. MPLA is derived either from LPS extracted from *Salmonella Minnesota* R595 strain or via chemical synthesis. Bacterial LPS-derived MPLA (Lipid A) comprises a heterogeneous population of tetra-, penta-, and hexa-acylated Lipid A molecules with varying acyl chain lengths, which contribute to differences in potency[14,29]. For example, tetra-acylated Lipid A exhibits lower TLR4 activation potential and may even act as an antagonist[30]. Compared to LPS, MPLA displays a significantly reduced immunostimulatory profile[31]. Efforts to create more potent and purified TLR4 agonists have led to the development of synthetic lipid A analogues for clinical use. These analogues, such as E6020, eritoran, aminoalkyl glucosaminide 4-phosphates (AGPs), and glucopyranosyl lipid A (GLA), are engineered without disaccharide backbones[31–34]. Further, when formulated with delivery systems like liposomes or oil-in-water emulsions, these analogues exhibit enhanced TLR4-mediated activity[35]. Recent studies have shown the development of a new class of Lipid A adjuvants by modification of MPLA at the 1st and 6th positions with α- and β-rhamnose (Rha), as well as a simplified lipid A analogue, GAP112, which have shown enhanced immunostimulatory activity with reduced endotoxicity, making them promising candidates for next-generation vaccine adjuvants[36,37]. However, Lipid A analogues, including MPLA, are challenging to synthesize and costly. Recent advancements in the discovery and development of synthetic small-molecule TLR agonist-based adjuvants have revolutionized vaccinology[38]. Examples include palmitoylated peptides and compounds such as pyrimido[5,4-b]indoles, imidazo[4,5-c]indoles, neoseptins, thiazoloquinolines, benzoazepines, and 8-oxoadenines, which activate TLR2, TLR4, TLR7, and TLR8[39–47]. These small molecules are not only easier to synthesize and cost-effective but also potent in eliciting balanced Th1/Th2 responses. Furthermore, they offer advantages such as ease of modification and derivatization

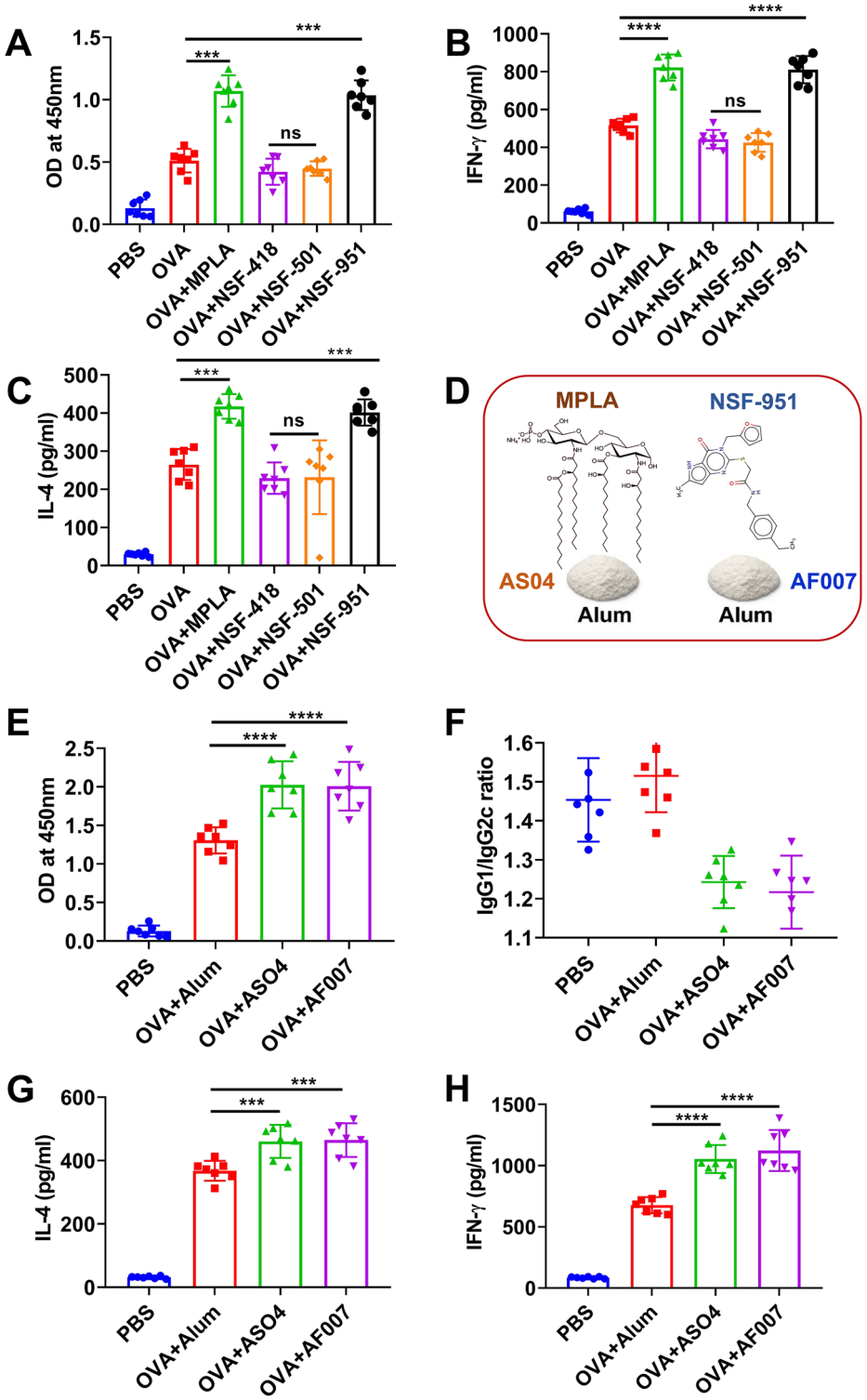

Fig. 5 | Adjuvant activity of NSF-951 in vivo. *Antigen specific immune response in mice immunized with OVA formulated with compounds.* Mice were immunized with OVA formulated in NSF-951 or NSF-418, or NSF-501 or MPLA, and antigen-specific Antibody response (**A**) in the serum obtained at day 28 was determined by ELISA and cellular immune response was determined by analysing the levels of IL-4 (**B**) and IFN-γ (**C**) in the culture supernatant of the stimulated spleenocytes using were analysed by ELISA as detailed in the materials and methods section and was determined as described in materials and methods. (Antigen-specific immune response in mice immunized with OVA formulated with AF007. **D** Pictorial combination of ASO4 (Alum +MPLA) and AF007 (Alum +NSF951). Mice were immunized with OVA formulated with Alum and NSF-951 (AF007) or MPLA (AS04), and antigen-specific Antibody response (**E**), Isotypes (**F**) in the serum obtained at day 28 was determined by ELISA and cellular immune response was determined by analysing the levels of IL-4 (**G**) and IFN-γ (**H**) in the culture supernatant. All experiments were performed in two independent biological replicates with four animals per group (n = 4). Data are presented as mean ± SD. Statistical significance was determined by one-way ANOVA followed by Dunnett's post hoc test. Significance is indicated as follows: $^{***}P < 0.001$, $^{****}P < 0.0001$, and ns (not significant).

for creating adjuvant-antigen complexes (self-adjuvanting vaccines) and optimized formulations[43,48,49]. The advancement of computational tools, such as computer-aided drug design (CADD), molecular docking and structure-based virtual screening (SBVS) and pharmacophore modelling, has significantly enhanced the discovery of potential TLR4-binding small molecules, either as agonists or antagonists[18,50,51]. Molecular dynamics simulations provide detailed insights into the stability and dynamics of TLR4-ligand interactions, improving prediction accuracy[52]. Machine learning methods further facilitate the prediction of ADMET (absorption, distribution, metabolism, excretion, and toxicity) properties, ensuring favourable pharmacokinetic and toxicological profiles for selected candidates[53,54]. These approaches leverage 3D molecular models and high-performance computing to screen and optimize compounds for binding affinity and efficacy[55,56].

Several therapeutic and prophylactic formulations that showed promising results in preclinical studies using mice often failed to demonstrate comparable potency in clinical settings. To address this issue, our in silico approach aimed to identify TLR4 agonists capable of inducing potent adjuvant activity across different host species. The goal was to ensure that the identified compounds or their formulations would have translational

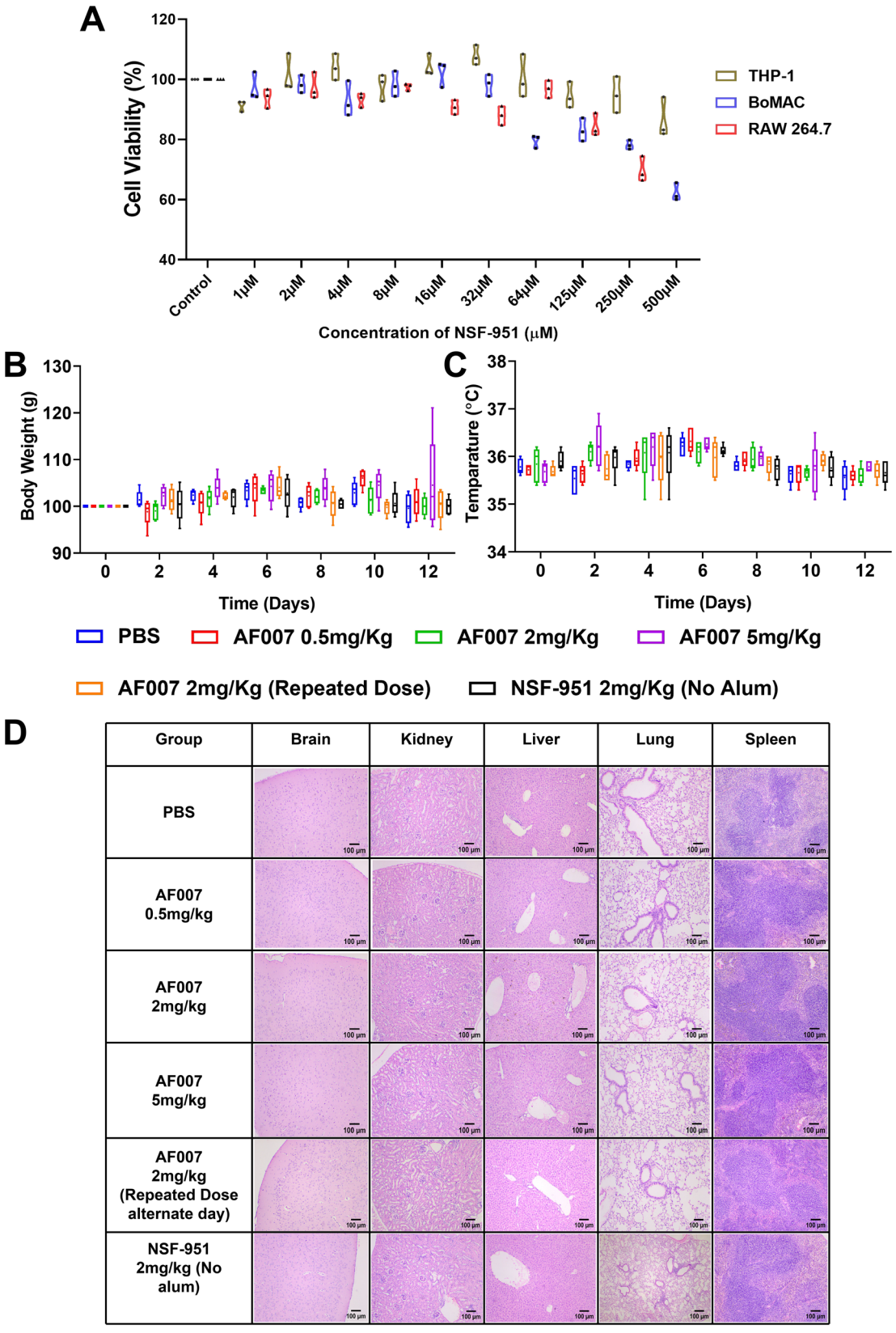

Fig. 6 | Evaluation of toxicity of NSF-951. A RAW 264.7, THP-1 and BoMac macrophage cell lines were treated with different concentrations (1μM- 500 μM) of the NSF-951 for 24 hrs at 37 °C/ 5%CO_2 and MTT assay was performed as described in materials and methods. Data represent mean ± SD from triplicate wells ($n = 3$), and are representative of two independent experiments. Toxicity of NSF-951 was evaluated both on the basis of the number of administrations viz., single dose (acute) or repeated dose(chronic) and amount viz. low dose and high dose. **B** Body weight (in grams) and **C** Body temperature (°C) were monitored till 12 days post injection. **D** *Histopathological analysis of vital organs*. Representative images of Hematoxylin and Eosin-stained tissues (brain, kidneys, liver, lungs and spleen) were obtained from various groups of animals at 12th day post treatment (scale bars, 100 μm). All in vivo experiments were conducted in two independent biological replicates, each comprising five animals per group ($n = 5$). Data are expressed as mean ± SD.

value and clinical applicability. Although TLR4 signalling pathways in mice and humans are similar, they are not identical. Species-specific differences in response to TLR4 ligands have been documented. For instance, the lipid A analogue lipid IVa acts as a TLR4 antagonist in humans but functions as a TLR4 agonist in mice[57]. These variations likely arise from subtle differences in the structure of TLR4 and its co-receptor MD2 between humans and mice. Considering these differences, our focus was on identifying compounds that exhibited strong binding to TLR4 receptors across various mammalian species, with binding energies comparable to or greater than those of MPLA. Based on additional criteria of predicted non-toxicity, ease of synthesis, or commercial availability, three small molecule (NSF-951, NSF-418, NSF-501) were identified with strong binding to TLR4-MD2, with NSF-951 showing superior affinity over MPLA, especially in mouse TLR4-MD2 (−8.5 vs −5.7 kcal/mol) (Fig. 1A, Table 1). Docking and MD simulations confirmed stable binding and favourable interactions of all three compounds within the TLR4-MD2 pocket, with NSF-951 maintaining strong dynamic stability (Fig.1B–D, Supplementary Fig. 2). SwissADME analysis further validated their drug-likeness of all compounds, highlighting NSF-951's balanced lipophilicity and oral bioavailability (Supplementary Table 2). While the in silico findings were compelling, it was essential to validate the adjuvant activity of these compounds through in vitro experiments and subsequent in vivo studies[58,59].

Our in vitro results indicate that while all three compounds (NSF-418, NSF-501, and NSF-951) demonstrated binding to TLR4-MD2, only synthetic NSF-951 effectively induced the activation and maturation of macrophages across different mammalian species. This was evident from the production of proinflammatory cytokines, increased expression of costimulatory molecules, and maturation markers (Fig. 2). Notably, NSF-951 exhibited potency at a dose much lower (in terms of mass) than MPLA (1763.469 g/mol) as being small molecule 1 μM NSF-951 (436.537 g/mol) corresponds to only 0.436 μg/mL, which is in fact lower than 2 μg/mL (1.13 μM), of MPLA (Supplementary Fig. 5D). Interestingly, NSF-951 although induced a dose dependent proinflammatory response upto 2 μM however it failed to enhance this response in macrophages beyond 2 μM, indicating a plateau rather than a decline in response (Supplementary Fig. 5C, E). This suggests saturation of TLR4 signalling, where maximal receptor and adaptor engagement limits further cytokine induction[9,60]. Such a plateau may be advantageous for adjuvant development, offering controlled immune activation without excessive inflammation. This mirrors the behaviour of MPLA, a clinically approved TLR4 agonist known to induce sufficient innate activation while minimizing systemic reactogenicity, key features of an ideal vaccine adjuvant[27,29]. The inability of NSF-951 to induce proinflammatory response in TLR4$^{-/-}$ macrophages confirms that it is a TLR4 agonist (Fig. 3A). To determine whether the TLR4 agonist activity of NSF compounds results from direct interaction with TLR4 or is mediated via MD-2, we performed MST assays using recombinant TLR4 in the absence of MD-2. While NSF-951 exhibited the strongest binding (K_D = 16.01 μM), NSF-418 and NSF-501 showed weaker affinities, and all compounds displayed large error margins. These results indicate that the NSF compounds do not bind TLR4 directly with high affinity, supporting prior in silico predictions that their activity is MD-2 dependent. MD-2 is a well-established co-receptor essential for ligand-induced TLR4 activation, with mutational studies showing that disruption of MD-2 impairs responsiveness to LPS and small-molecule agonists[61,62]. Notably, compounds such as L6H21 inhibit TLR4 signalling by binding MD-2 rather than the TLR4 LRR domain[61].Our findings suggest that NSF-951 likely targets hydrophobic pockets within MD-2, consistent with computational docking models. Taken together, these data support the hypothesis that the agonistic activity of NSF compounds is not due to direct TLR4 binding but rather to specific interactions with MD-2. This mechanistic insight has important implications for the design and screening of small-molecule TLR4 agonists. Our MST-based results underscore the limitations of studying TLR4-targeted ligands using the LRR domain alone and highlight the necessity of including MD-2 in future biophysical and functional assays[63]. Combined with MST data suggesting low micromolar affinity for TLR4, the EC_{50} value reinforces the hypothesis that NSF-951 may exert its activity through MD-2-dependent engagement within the TLR4–MD-2 complex. These findings provide a foundation for further preclinical evaluation of NSF-951 as a synthetic immunomodulator, particularly in the context of innate immune activation or adjuvant applications. The small molecules NSF-418 and NSF-501, despite their predicted binding to TLR4-MD2, failed to exhibit agonist activity in macrophages from any tested species (Fig. 2 and Supplementary Fig. 5A, B). This suggests that these compounds might function as antagonists. Supporting this hypothesis, our results show that both synthetic NSF-418 and NSF-501 antagonized MPLA-induced proinflammatory responses in mouse macrophages (Fig. 3B), consistent with previously identified small-molecule TLR4 antagonists[64]. It is not surprising that the sequential addition of NSF-951 followed by MPLA did not enhance cytokine production compared to MPLA alone (Fig. 3B). This may be due to the moderate binding affinity of NSF-951 with TLR4/MD-2 complex, causing partial internalization or altering its conformation, reducing MPLA's effectiveness when added later. Further, pretreatment with NSF-951 could initiate low levels of TLR4 engagement or receptor internalization, leading to a transient refractory state when MPLA is subsequently added. This phenomenon, often referred to as endotoxin tolerance or ligand-induced hypo responsiveness, is well-documented in innate immune signalling, especially in the context of repeated or sequential TLR stimulation[65,66]. Thus, despite MPLA's potency, prior exposure to NSF-951 may limit the cell's ability to mount a fully additive or synergistic cytokine response (Fig. 3B). Given that TLR4 signalling via LPS predominantly involves the MyD88 pathway, while MPLA is TRIF-biased, we sought to determine the adapter pathway utilized by NSF-951[10]. Our findings reveal that, NSF-951 induces signalling through both MyD88 and TRIF adapters. This was evident from the reduced cytokine production in MyD88 knockout macrophages and the induction of TRIF-associated factors such as IFN-β, MCP-1, IP-10, and RANTES (Fig. 4A, B). Previous studies have demonstrated that certain TLR4 ligands can utilize both MyD88 and TRIF pathways synergistically to induce proinflammatory cytokines[67,68]. It is important to note that the chemical structure of TLR4 modulators plays a crucial role in pathway activation. For example, MPLA, a large and complex molecule, preferentially activates TRIF, skewing lymphocytes toward a Th1 response. In contrast, small molecules like 1Z105 bias TLR4 signalling through MyD88, promoting a Th2 response[69]. It would be interesting to observe if CD14 is dispensable for NSF-951-mediated TRIF signalling, as prior studies have shown that MPLA and small molecules like UT-2, 1Z105, and Ugi compounds mediate TLR4 stimulation independent of CD14[41,52]. Interestingly, compounds like UT-2 and 1Z105 bypass CD14 for ligand transfer or TLR4/MD2 complex internalization, likely due to their ability to bind MD2 directly. Our docking results suggest that NSF-951 similarly binds directly to MD2, potentially compensating for the role of CD14 (Fig. 1B, C). However, due to lack of CD14 knockout cell line we could not confirm the role of CD14 in NSF-951 mediated signalling. Finally, we examined the involvement of MAP kinase signalling pathways, including p38, ERK, and JNK, which regulate inflammatory cytokine expression. Our findings indicate that NSF-951 induces activation via the p38 and JNK pathways, as evidenced by their phosphorylation and the inhibition of cytokine production by specific pharmacological inhibitors (Fig. 4C, D). This behaviour of NSF-951 is somewhat distinct from MPLA, which has been shown to induce strong p38 activation but weak JNK activation[70].

To evaluate the adjuvant activity of NSF-951 In vivo, we formulated OVA with NSF-951, MPLA, or TLR4 antagonists (NSF-501 and NSF-418) and immunized mice to assess OVA-specific antibody and T-cell responses. Our results demonstrated that NSF-951 significantly enhanced OVA-specific IgG production and T-cell responses, as indicated by higher levels of IL-4 and IFN-γ (Fig. 5). This aligns with previous studies showing that several small-molecule TLR4 agonists identified through high-

throughput in vitro screening can enhance immune responses against various antigens[71–73]. Similar to MPLA, NSF-951 is an immunostimulatory molecule and lacks inherent antigen-delivery properties. Thus, formulating it with delivery systems or co-adjuvants, such as Alum, liposomes, microparticles, or oil emulsions, is expected to enhance its adjuvant activity. For instance, MPLA formulated with Alum (AS04), liposomes (AS01), or oil emulsions (AS03) has demonstrated potent adjuvant effects, with some formulations already in clinical use[74–77]. Based on these reports, we tested the adjuvant activity of an Alum formulation with NSF-951, termed AF007. Our results revealed that AF007 showed potency comparable to AS04, although the dose of NSF-951 was similar to MPLA (Fig. 5). Increasing the dose of NSF-951 in the AF007 formulation could enhance the immune response; however, this needs to be tested further. Extensive evaluation of the AF007 formulation with bacterial and viral antigens is required to determine its ability to induce long-term memory responses and efficacy against disease in animal models. Establishing AF007 as a potential alternative to AS04 could provide a cost-effective option, given that NSF-951 synthesis is easier and cheaper than MPLA.

A critical concern in adjuvant development is reactogenicity and toxicity, as several adjuvants that showed potency in preclinical studies were associated with mild to moderate toxicity[78]. Therefore, adjuvants must demonstrate both efficacy and safety for vaccine development. Our in vitro and in vivo toxicity studies indicate that NSF-951 did not induce significant toxicity in different species of macrophage cell lines and in acute or chronic toxicity tests in mice model (Fig. 6). No acute inflammatory events, either localized (inflammation, redness, tenderness) or systemic (fever), were observed, and no lesions were detected in vital organs (Fig. 6). At higher doses, when administered alone or with Alum, NSF-951 induced dose-dependent histopathological changes, particularly in the liver and spleen (Supplementary Fig. 11). Mild pigmentation at a dose of 0.5 mg/kg suggested early signs of hemosiderin accumulation, likely related to immune response-induced alterations in iron metabolism[79,80]. Additionally, mild hypertrophy of splenic lymphatic follicles at a dose of 2 mg/kg in some animals suggests an immunostimulatory/adjuvant effect of NSF-951[81,82] (Supplementary Fig. 11). These tissue changes, including increased cellular activity and inflammatory responses, were attributed to immune cell activation. The absence of severe damage indicates that the immune response was localized and controlled. However, further research is needed to elucidate the mechanisms underlying these tissue changes and to optimize NSF-951 for maximal efficacy with minimal adverse effects.

In summary, using an in silico approach, we identified a small-molecule TLR4 agonist, NSF-951, which has demonstrated strong adjuvant activity without causing significant reactogenicity or toxicity. To evaluate the mechanism of NSF-951 binding to mTLR4-MD2, site-directed in silico mutagenesis was employed, which not only identified critical residues mediating ligand interaction but also predicted the binding pocket, consistent with prior alanine-scanning studies that elucidated receptor-ligand interfaces[83]. NSF-951 has not been shown to be associated with any other biological activity (antimicrobial, anti-inflammatory, anti-cancer) as revealed by PubChem search engine. NSF-951 and its formulation with Alum (AF007) have been filed for patent. It is important to note that MPLA requires complex multi-step synthesis and rigorous purification processes due to its lipid-based, amphiphilic structure and stereochemistry. As compared to MPLA, NSF-951 is much simpler to synthesize involving fewer steps and utilizing commercially available starting materials. Moreover, it does not require lipid conjugation or enzymatic processing thus reducing the technical complexity, time, and cost associated with production. Based on laboratory-scale synthesis estimates, the cost of production for NSF-51 is expected to be at least threefold lower than that of MPLA, making it a more accessible and cost-effective adjuvant, especially for animal vaccines. Future studies should evaluate the adjuvanticity of NSF-951 formulated with bacterial and viral antigens, alongside additional co-adjuvants, and compare its potency and safety with existing clinical adjuvants.

Materials and Methods

Identification and characterization of TLR4 binding compounds in silico

For virtual screening, a ligand library of natural products and economically purchasable compounds was downloaded from the ZINC database (https://zinc.docking.org/substances/subsets/natural-products/) using a Linux-based Dell workstation in mol2 format[84]. Following the standard protocols of AutoDock Tools, biological targets (receptors) were processed, including hTLR4-MD2 (PDB ID: 4G8A for *Homo sapiens*), bTLR4-MD2 (PDB ID: 3RG1 for *Bos taurus*), and mTLR4-MD2 (PDB ID: 3T6Q for *Mus musculus*)[85]. These receptor structures were downloaded from the Protein Data Bank (https://www.rcsb.org/). The receptors were converted into PDBQT format by removing all water molecules, adding only polar hydrogen atoms, and incorporating Kollman charges. The prepared files were saved for further processing. Ligands from above small molecules were filtered to exclude aromatic compounds and downloaded in SMILES (.smi format) and converted to mol2 and then in SDF in 3D format and finally in PDB format using Open Babel software. Further conversion into PDBQT format was followed by filtering using Lipinski's Rule of Five (logP <5, molecular weight <500 Da, ≤10 H-bond acceptors, and ≤5 H-bond donors) as described previously[86,87]. Duplicate ligands were discarded. The unique ligands were docked into the active site of hTLR4-MD2, bTLR4-MD2, and mTLR4-MD2 using AutoDock Vina (version 1.1.2), estimating their binding energies. The docking focused on the binding pockets of TLR4-MD2 where the known agonist MPLA binds, with grid box values and coordinates provided in Supplementary Table 1. Inputs for the compounds were automated using an in-house Perl script ("autodock_vina_parallel.pl"), combining the affinity results. The structure-based virtual screening was completed using the command line to optimize CPU usage and reduce processing time. Compounds were ranked based on their binding scores. A detailed pipeline of the procedure is illustrated in Supplementary Fig. 1. The selected compounds were further analyzed for pharmacokinetic properties, including absorption, distribution, metabolism, excretion, and toxicity (ADMET), using the SwissADME tool (http://www.swissadme.ch/) and admetSAR2 (https://lmmd.ecust.edu.cn/admetsar2/). Further to confirm the ligand-receptor interactions, in silico mutagenesis of critical residues inside the mTLR4-MD2 binding pockets were conducted through mutagenesis wizard using PyMOL. The mutant receptors were converted into PDBQT format utilising the identical AutoDockTools method. The mutant receptors were subsequently re-docked with NSF-951 utilising AutoDock Vina, applying the same grid coordinates and docking parameters as those employed for the wild-type mTLR4-MD2 (3T6Q) structures.

Procurement of compounds, cell lines, and reagents

The compounds NSF-951, NSF-408, and NSF-501 were procured as solid powders from Molport, USA. These compounds were dissolved in dimethyl sulfoxide (DMSO) (Sigma-Aldrich, St. Louis, MO) to prepare stock solution of 10 mM and stored at −20 °C. The cell lines used in this study included the mouse macrophage cell line RAW264.7, the human monocytic cell line THP1, all of which were purchased from the American Type Culture Collection (ATCC, Manassas, VA). Additional mouse macrophage cell lines —Wild Type (WT; NR-9456), $TLR4^{-/-}$(NR-9458), $TRIF^{-/-}$ (NR-9566), $MyD88^{-/-}$ (NR-15633), $MyD88^{-/-}TRIF^{-/-}$(NR-15632)—were obtained from BEI Resources, USA. BoMac cells were kindly provided by Dr. Judy Stabel (Johne's Disease Research Project, USDA-ARS-NADC). RAW264.7 and mouse knockout macrophage cells were cultured in DMEM, while THP1 and BoMac cells were cultured in RPMI-1640 (Sigma, USA), supplemented with 10% FBS (Invitrogen, Carlsbad, CA, USA), 100 U/mL penicillin, and 100 mg/mL streptomycin. All cell cultures were maintained at 37 °C in a humidified incubator with 5% CO_2. Inhibitors targeting NF-κB (SN50), p38 (SB203580), MEK1/MEK2 (U0126), and JNK (SP600125) were purchased from Invivogen. Recombinant mouse TLR4 (9149-TR), cytokine estimation kits for mouse, human, and bovine IL-6 and TNF-α were

obtained from R&D Biosystems. Monolith Protein Labelling Kit RED-NHS (NanoTemper Technologies) for labelling mTLR4. Antibodies for flow cytometry experiments, including PerCP-Cy5.5–conjugated anti-mouse MHC-II (562363), APC-conjugated anti-mouse CD80 (560016), and PE-conjugated anti-mouse CD86 (553692), were procured from BD Biosciences, USA. Monophosphoryl Lipid-A and Alhydrogel® and ovalbumin were purchased from Invivogen. Unless otherwise stated, all other reagents were obtained from Sigma.

Animals

Male C57BL/6 mice (5–6 weeks old) were obtained from the Animal Resource and Experimental Facility of the Institute. The animals were maintained under standard pathogen-free conditions, with access to food and water *ad libitum*. All experimental procedures involving mice were performed in accordance with the guidelines of the Institutional Animal Ethics Committee (IAEC) and were approved under protocol number IAEC/NIAB/2023/42/SF. For bovine blood collection, six-year-old female Dangi cattle housed at the Large Animal Farm Facility of the Institute were used. All procedures involving cattle were conducted in compliance with IAEC guidelines and were approved under protocol number IAEC/NIAB/2023/44/SF. We have complied with all relevant ethical regulations for animal use.

Cell stimulation assays

RAW264.7 cells (1×10^6 cells per well) were cultured in complete DMEM medium and stimulated with various concentrations ranging from 0.2 μM to 20 μM) of compounds NSF-418 or NSF-501 or NSF-951 for 24 hours at 37 °C in a 5% CO_2 environment. Cells treated with MPLA (2 μg/mL, ~1.13 μM) served as positive controls, while those treated with medium alone served as negative controls. THP-1 cells (1×10^6 cells per well) were cultured in complete RPMI 1640 medium and treated with 10 ng/mL phorbol 12-myristate 12-acetate (PMA) for two days at 37 °C in 5% CO_2 to induce differentiation into macrophages. After two days, the PMA-containing media was removed, fresh complete media was added, and the cells were incubated for an additional 24 hours. Differentiated THP-1 macrophages were stimulated with 2 μg/mL MPLA (1.13 μM), or 2 μM of NSF-418(0.679 μg/mL) or NSF-501(0.649 μg/mL) or NSF-951 (0.873 μg/mL) for 24 hours at 37 °C in 5% CO_2. BoMac cells (1×10^6 cells per well) were cultured in complete RPMI 1640 medium and stimulated with MPLA (2 μg/mL), or 2 μM of NSF-418 or NSF-501 or NSF-951 for 24 hours at 37 °C in 5% CO_2. To assess antagonist activity, RAW264.7 cells (1×10^6 cells per well) were pre-treated with 2 μM of NSF-418 or NSF-501 or NSF-951 before stimulation with MPLA (2 μg/mL). Cytokine levels in the culture supernatant were measured using sandwich ELISA kits. In a separate experiment, 1×10^6 cells per well of Mouse WT, TLR4$^{-/-}$, TRIF$^{-/-}$, MyD88$^{-/-}$, and MyD88$^{-/-}$TRIF$^{-/-}$cell lines were stimulated with MPLA (2 μg/mL), or 2 μM of NSF-418 or NSF-501 or NSF-951 for 24 hours at 37 °C in 5% CO_2. To access the signalling pathway involved, additional experiments were done in which RAW264.7 cells were pre-treated with specific inhibitors for 30 minutes at 37 °C in 5% CO_2: NF-κB inhibitor (520 μM), JNK inhibitor (40 μM), MEK1/2 inhibitor (25 μM), or p38 inhibitor (230 μM). Cells were then stimulated with MPLA (2 μg/mL), or 2 μM of NSF-418 or NSF-501 or NSF-951 for 24 hours at 37 °C in 5% CO_2. Culture supernatants from above stimulated cells (RAW264.7, BoMac, THP-1, WT, TLR4$^{-/-}$, TRIF$^{-/-}$, MyD88$^{-/-}$, and MyD88$^{-/-}$TRIF$^{-/-}$) were collected after 24 hours of stimulation.

Cytokine ELISA

The levels of interleukin-6 (IL-6) and tumour necrosis factor-alpha (TNF-α) in the culture supernatants of were quantified using a standard sandwich enzyme-linked immunosorbent assay (ELISA). Briefly, A 96-well flat-bottom ELISA plates were coated overnight at 4 °C with capture antibodies specific to host IL-6 or TNF-α (R&D Systems), diluted in phosphate-buffered saline (PBS). Following the coating process, plates underwent three washes with PBS supplemented with 0.05% Tween-20 (PBST) and were subsequently blocked with 1% bovine serum albumin (BSA) in PBS for one hour at room temperature to mitigate nonspecific binding. Subsequent to the blocking step, 100 μL of cell culture supernatants were introduced into the wells in duplicate and incubated for 2 hours at room temperature. Plates were washed thoroughly with PBST three times, after which biotinylated detection antibodies specific to each cytokine were added to the appropriate wells and incubated for 2 hours. Following three washes, streptavidin-horseradish peroxidase (HRP) conjugate was introduced and incubated for 30 minutes. Subsequently, wash with PBST three times. The enzymatic reaction was initiated by the addition of 100 μL of tetramethylbenzidine (TMB, MP Biomedicals) substrate solution, followed by a 20-minute incubation in the dark. The reaction was terminated by the addition of 50 μL of 2 N H_2SO_4, and the optical density was assessed at 450 nm with a reference wavelength of 540 nm utilising an ELISA reader (Perkin Elmer). The concentrations of cytokines in the samples were determined using standard curves established from known concentrations of recombinant IL-6 and TNF-α.

In vitro binding evaluation of TLR4 ligands via MST

Microscale thermophoresis (MST) was employed to assess potential direct binding interactions between the small molecules NSF-418, NSF-501, NSF-951, and mouse Toll-like receptor 4 (TLR4) using modified protocol published previously[88]. Briefly, recombinant mouse TLR4 protein (R&D Systems, Minneapolis, MN) was fluorescently labelled using the Monolith NT™ Protein Labelling Kit RED-NHS (NanoTemper Technologies, Germany) according to the manufacturer's protocol (NanoTemper Technologies, 2021). Labelling was performed in the provided buffer, and the labelled protein was subsequently eluted into 1× phosphate-buffered saline (PBS; pH 7.4). MST binding assays were conducted using 35 nM NT647-labelled TLR4 in assay buffer containing 50 mM Tris-HCl, 150 mM NaCl, 10 mM $MgCl_2$, and 0.05% Tween-20 (pH 7.4). The small molecules NSF-418, NSF-501, and NSF-951 were tested at the range of 500 μM to 0.244 μM, while monophosphoryl lipid A (MPLA), a known TLR4 agonist, was tested at the range 250 μM to 0.122 μM. Samples were loaded into standard capillaries and analyzed on a Monolith NT.115 Pico instrument (NanoTemper Technologies, Munich, Germany) at 25 °C, with 100% LED power and medium MST power. Each measurement was performed in triplicate. Thermophoretic movement was monitored over 20 seconds, capturing both the temperature jump (T-jump) and thermophoresis phases. The dissociation constant (K_D) values and their confidence intervals were determined using MO. Affinity Analysis v2.3.

qRT-PCR

RAW264.7 or TRIF$^{-/-}$ or THP-1 or BoMac cell lines were seeded (1×10^6 cells per well) into 6-well plates and treated with MPLA (2 μg/mL), or 2 μM of NSF-418 or NSF-501 or NSF-951 for 24 hours at 37 °C in 5% CO_2. Following treatment, RNA was purified using the Nucleospin RNA purification Kit (MN) as per the manufacturer's protocol. 1 μg RNA was reverse transcribed using PrimeScript 1st strand cDNA Synthesis Kit (Takara, Japan). Quantitative Real-time PCR (qRT-PCR) was performed using specific primers (Supp Table 3). For PCR, SYBR Green PCR-Master mix (iTaq™ Universal SYBR Green, Bio-Rad, USA) was used with cycling conditions: initial step at 95 °C for 30 s, followed by 40 cycles of 95 °C for 5 s and 60 °C for 30 s, using CFX96 Touch Real-Time PCR Detection System (Bio-Rad, USA). Experimental data are presented as $\log_2$ fold changes in gene expression relative to controls. mRNA levels were normalized to GAPDH expression.

Flow cytometry analysis

RAW264.7 cells (1×10^6 cells per well) were stimulated with MPLA (2 μg/mL), or 2 μM of NSF-418 or NSF-501 or NSF-951 for 24 hours at 37 °C in a 5% CO_2 environment. After incubation, cells were harvested, washed with pre-chilled PBS, and blocked using a blocking solution containing 0.5% BSA and 2% FBS in PBS for 30 minutes. Following three washes with PBS, cells

were incubated for 1 hour on ice in the dark with 2.5 µg PerCP-CY5.5–conjugated anti-MHCII, APC-conjugated CD80, and PE-conjugated CD86 antibodies per million cells (BD Biosciences, USA). After incubation, cells were washed, fixed with 1% paraformaldehyde, and 50,000 total events per sample were acquired using a BD LSR Fortessa flow cytometer. Data were analyzed using FlowJo (v10.8.1) software.

Western blot analysis

RAW264.7 cells (1×10^6 cells per well) were stimulated with MPLA (2 µg/mL), or 2 µM of NSF-418, NSF-501, NSF-951 for 24 h at 37 °C under 5% CO_2. Treated cells were collected and lysed with RIPA cell lysis buffer supplemented with a cocktail of protease and phosphatase inhibitors (Sigma Aldrich). The lysates were centrifuged at 12,000 × *g* for 30 minutes at 4 °C, and protein concentrations in the supernatant were measured using a BCA protein quantification assay (ChemCruz). Equal amounts of protein were separated by 10% SDS-PAGE and transferred onto PVDF membranes (0.22 µm; Millipore, Bedford, MA). Membranes were blocked with 5% BSA in Tris-buffered saline containing 0.1% Tween-20 (TBST; pH 7.4) and incubated overnight at 4 °C with primary antibodies diluted 1:1000, including anti-p38 (sc-728), anti-phospho-p38 (sc-17852-R), anti-ERK (sc-153), anti-phospho-ERK (sc-23759-R), anti-SAPK/JNK (sc-571), anti-phospho-SAPK/JNK (sc-12882-R), and GAPDH (sc-365062) from Santa Cruz Biotechnology. After three washes with TBST (0.1% Tween-20), membranes were incubated with 1:3000 HRP-conjugated anti-rabbit (7074S) or anti-mouse IgG (7076S) for 1 hour at room temperature. GAPDH was used as a loading control to ensure equal protein loading. Protein bands were visualized using Clarity™ Western ECL substrate (BioRad) in ChemiDoc System (BioRad).

Generation of mouse bone marrow-derived dendritic cells (BMDCs)

Mouse bone marrow-derived dendritic cells (BMDCs) were generated following a previously described protocol[89]. Bone marrow cells were harvested from the femurs and tibias of mice and filtered through a 70 µm cell strainer into a sterile culture dish containing complete DMEM medium. The cell suspension was centrifuged at 1000 rpm for 5 minutes, and the supernatant was discarded. Red blood cells were lysed using ACK lysis buffer, followed by three washes with PBS. The remaining cells were resuspended in complete DMEM medium. Bone marrow cells (1×10^7 cells per well) were seeded in 6-well plates with 4 mL of complete DMEM medium supplemented with GM-CSF (20 ng/mL) and IL-4 (5 ng/mL) (Peprotech). On days 2 and 7, half of the medium was replaced with fresh medium containing GM-CSF (40 ng/mL) and IL-4 (10 ng/mL). On day 9, non-adherent and loosely adherent cells were removed, and adherent cells were harvested via gentle PBS washing. The harvested cells were pooled and used for subsequent assays.

Isolation of bovine PBMCs

Bovine peripheral blood mononuclear cells (PBMCs) were isolated using a standard density gradient centrifugation method. Briefly, blood samples were collected from cattle into EDTA-coated tubes and diluted 1:1 with phosphate-buffered saline (PBS). The diluted blood was gently layered over Histopaque®−1077 (Merck, Cat. No. 10771-100 ML) in 50 mL conical centrifuge tubes. Samples were centrifuged at 400 × *g* for 30 minutes at room temperature without applying the brake. Following centrifugation, the mononuclear cell layer (buffy coat) was carefully aspirated, washed with RPMI-1640 medium, and resuspended in complete RPMI-1640 supplemented with 10% foetal bovine serum and antibiotics. The isolated cells were counted and subsequently used for downstream immunological assays.

MTT assay

The MTT assay was performed following a previously published protocol[90]. A 5 mg/mL solution of 3-(4,5-dimethylthiazol-2-yl)−2,5-diphenyltetrazolium bromide (MTT, Product Number M2128) was prepared in PBS and filter-sterilized. RAW264.7/BoMac/THP-1 cells (10,000, 20,000 and 50,000 cells/well, respectively) were seeded into a 96-well flat-bottom plate and treated with varying concentrations (1 µM to 500 µM) of NSF-951 or NSF-418 or NSF-501 and plates were incubated at 37 °C in a 5% CO_2. Cells treated with 10% Triton X-100 served as the positive control, while untreated cells served as the negative control. After 24 hrs for incubation, 20 µL of the MTT solution was added to each well, and the plates were incubated for an additional 3.5 hours. After incubation, the media were carefully removed, and 150 µL of MTT solvent (DMSO) was added to each well. The plates were covered with foil and agitated on an orbital shaker for 15 minutes to dissolve the MTT formazan crystals. Absorbance was measured at 590 nm with a reference filter at 620 nm.

Preparation of antigen, adjuvant and vaccine formulation

Chicken ovalbumin (OVA), used as the model antigen, was reconstituted in endotoxin-free water (Millipore) at a concentration of 1 mg/mL and stored at −20 °C. 1 mg of NSF-951 or NSF-418 or NSF-501 powder was dissolved in a minimum volume of DMSO, followed by the addition of PBS to make a stock of 1 mg/mL. MPLA was prepared asa stock of 1 mg/mL solution in DMSO. For a single mouse formulation (injection volume: 100 µL) the formulation was prepared as follows- (a) Without Alum**:** 5 µL (5 µg) of OVA was added to 90 µL of PBS, followed by addition of 5 µL (5 µg) of MPLA or 5 µL (5 µg) of NSF-951/ NSF-418/NSF-501 to make 100 µL total volume. The mixture was gently pipetted and injected immediately. (b) With Alum**:** 5 µL (5 µg) of antigen was added to 40 µL of PBS, followed by addition of 5 µL (5 µg) of MPLA or 5 µL (5 µg) of NSF-951 to make 50 µL total volume. The mixture was gently pipetted, and 50 µL (500 µg) of Alum was added. The final solution was mixed gently and injected immediately or stored at 4 °C until use.

Animal immunizations and sample collection

Male C57BL/6 mice (five animals per group) were anesthetized with Isoflurane through the open drop method. Briefly, a cotton pad was soaked with a few drops of Isoflurane and then placed in a small container under a wire mesh. The animals were then placed in the container and the lids were tightly closed. The animals were monitored closely and the effect of anaesthesia was confirmed by the lack of a righting reflex when the jar is tipped slightly and a reduction in respiratory rate. The animals were allowed to remain in deep anaesthesia for ~10 sec and then immunized subcutaneously with 100 µL of PBS or PBS + OVA(5 µg) or PBS + OVA(5 µg)+MPLA(5 µg) or PBS + OVA(5 µg)+NSF-418(5 µg) or PBS + OVA(5 µg)+NSF-501(5 µg) or PBS + OVA(5 µg)+NSF-951(5 µg) or PBS + OVA(5 µg)+Alum(500 µg) or PBS + OVA(5 µg)+ AS04 [Alum(500 µg)+MPLA(5 µg)] or PBS + OVA(5 µg)+ AF007 [Alum(500 µg)+NSF-951(5 µg)]. Mice were boosted on day 21 and blood samples were collected before immunization (pre-bleed), one week after the booster dose, and at the endpoint (day 28). On day 28, the mice were euthanized by exposing the animals to CO_2 in a euthanasia chamber until complete cessation of breathing is observed for a minimum of 2 minutes. The blood and spleen samples were then collected to analyse antigen-specific antibody and T-cell responses.

Analysis of antibody response

The antibody levels in serum samples obtained from immunized mice were assessed using ELISA, following our previously published protocol[91]. Briefly, 96-well microtiter plates (Nunc, Denmark) were coated with OVA (100 ng/well) dissolved in 0.1 M bicarbonate buffer and incubated overnight at 4 °C. The following day, plates were washed three times with PBS containing 0.05% Tween 20 (PBST) and blocked with 1% BSA for 1 hour at room temperature. After blocking, plates were washed, and 100 µL of serially diluted serum samples (1:100 to 1:100,000 in PBS containing 1% BSA) were added to each well. The plates were incubated for 2 hours at 37 °C in a humidified chamber. Post-incubation, plates were washed, and 100 µL/well of HRP-conjugated goat anti-mouse IgG (1036-05, SouthernBiotech) or IgG1 (1071-05, SouthernBiotech) or

IgG2c (1078-05, SouthernBiotech) diluted 1:6,000 was added, followed by incubation at room temperature for 1 hour. After five additional washes, 100 µL of TMB substrate was added to each well and incubated in the dark at room temperature for 20 minutes. The reaction was stopped by adding 50 µL of 2 N H_2SO_4, and optical density was measured at 450 nm with a reference wavelength of 540 nm using an ELISA reader (Perkin Elmer).

Analysis of T-cell response

Spleens collected from each group of animals were processed into single-cell suspensions by passing the tissue through a 70 µm cell strainer. Red blood cells (RBCs) were lysed using ACK lysis buffer, and the resulting lymphocytes were seeded into 24-well plates at a density of 1×10^5 cells/well. The cells were then stimulated with 2 µg/mL of OVA and incubated for 48 hours. Cytokine levels of IL-4 and IFN-γ in the culture supernatants were measured using sandwich ELISA kits (R&D Systems), following the manufacturer's instructions.

Evaluation of in vivo toxicity

The toxicity of NSF-951 was assessed based on dosing regimen (single-dose acute or repeated-dose chronic) and dosage levels (low and high), following a previously described protocol[92]. Toxicity evaluations included both local and systemic parameters. The animals were monitored for food intake, body weight, body temperature, general behaviour such as hyperactivity/lethargy/aggressiveness etc. Physical examination, including observations of hair coat, salivation, eye prominence, eyelid closure, tremors etc. was monitored twice a week. The neurological examination, including tail elevation, abnormal ataxic gait, head position, pinna touch response etc., was also recorded at least twice a week. Animals were euthanized and a necropsy was performed to examine internal abnormalities, particularly lymph node enlargement. Internal organs (liver, spleen, kidneys, lungs, brain) were examined for gross morphological changes, weighed, and preserved in 10% neutral-buffered formalin. The tissue samples were processed using conventional histological methods. Paraffin sections (5 µm thick) were stained with hematoxylin and eosin and examined under a light microscope by a board-certified pathologist who was blinded to the treatment groups.

Statistics and reproducibility

Data from experiments were analyzed using one-way or two-way analysis of variance (ANOVA), followed by the Dunnett post hoc test unless stated otherwise. Results were presented as the mean ± standard deviation (SD) from duplicate or triplicate experiments as indicated. A p-value of less than 0.05 ($p < 0.05$) was considered statistically significant.

Reporting summary

Further information on research design is available in the Nature Portfolio Reporting Summary linked to this article.

Data availability

All relevant data supporting the findings of this study are available within the paper and its Supplementary Information files. Source data for all graphs and quantitative analyses, including raw values for ELISA, qRT-PCR, and other experimental readouts, are provided as raw data files in the Supplementary Information. These files contain the exact numerical data used to generate the figures and statistical analyses presented in the manuscript. Any additional data that support the conclusions of this study are available from the corresponding author upon reasonable request.

Code availability

The custom Perl script used for parallel batch docking with AutoDock Vina is available at: https://github.com/GCBL-NIAB/Parallel-Docking The repository includes the script, example input files, and usage instructions. The code is freely available without restrictions.

Received: 8 January 2025; Accepted: 23 July 2025;
Published online: 29 September 2025

References

1. Zhao, T. et al. Vaccine adjuvants: mechanisms and platforms. *Signal. Transduct. Target. Ther.* **8**, 283 (2023).
2. Reed, S. G., Orr, M. T. & Fox, C. B. Key roles of adjuvants in modern vaccines. *Nat. Med.* **19**, 1597–1608 (2013).
3. Facciola, A., Visalli, G., Lagana, A. & Di Pietro, A. An overview of vaccine adjuvants: current evidence and future perspectives. *Vaccines* **10**, https://doi.org/10.3390/vaccines10050819 (2022).
4. Mogensen, T. H. Pathogen recognition and inflammatory signaling in innate immune defenses. *Clin. Microbiol. Rev.* **22**, 240–273 (2009). Table of Contents.
5. Akira, S., Uematsu, S. & Takeuchi, O. Pathogen recognition and innate immunity. *Cell* **124**, 783–801 (2006).
6. Kawai, T. & Akira, S. The role of pattern-recognition receptors in innate immunity: update on Toll-like receptors. *Nat. Immunol.* **11**, 373–384 (2010).
7. Duan, T., Du, Y., Xing, C., Wang, H. Y. & Wang, R. F. Toll-like receptor signaling and its role in cell-mediated immunity. *Front. Immunol.* **13**, 812774 (2022).
8. Ciesielska, A., Matyjek, M. & Kwiatkowska, K. TLR4 and CD14 trafficking and its influence on LPS-induced pro-inflammatory signaling. *Cell. Mol. Life Sci.* **78**, 1233–1261 (2021).
9. Kagan, J. C. et al. TRAM couples endocytosis of Toll-like receptor 4 to the induction of interferon-beta. *Nat. Immunol.* **9**, 361–368 (2008).
10. Mata-Haro, V. et al. The vaccine adjuvant monophosphoryl lipid A as a TRIF-biased agonist of TLR4. *Science* **316**, 1628–1632 (2007).
11. Arias, M. A. et al. Glucopyranosyl Lipid Adjuvant (GLA), a Synthetic TLR4 agonist, promotes potent systemic and mucosal responses to intranasal immunization with HIVgp140. *PLoS One* **7**, e41144 (2012).
12. Verma, S. K. et al. New-age vaccine adjuvants, their development, and future perspective. *Front. Immunol.* **14**, 1043109 (2023).
13. Vandepapeliere, P. et al. Vaccine adjuvant systems containing monophosphoryl lipid A and QS21 induce strong and persistent humoral and T cell responses against hepatitis B surface antigen in healthy adult volunteers. *Vaccine* **26**, 1375–1386 (2008).
14. Wang, Y. Q., Bazin-Lee, H., Evans, J. T., Casella, C. R. & Mitchell, T. C. MPL adjuvant contains competitive antagonists of human TLR4. *Front. Immunol.* **11**, 577823 (2020).
15. Yang, J. X. et al. Recent advances in the development of toll-like receptor agonist-based vaccine adjuvants for infectious diseases. *Pharmaceutics* **14**, https://doi.org/10.3390/pharmaceutics14020423 (2022).
16. Romerio, A. et al. New Glucosamine-based TLR4 agonists: design, synthesis, mechanism of action, and in vivo activity as vaccine adjuvants. *J. Med. Chem.* **66**, 3010–3029 (2023).
17. Shukla, N. M., Chan, M., Hayashi, T., Carson, D. A. & Cottam, H. B. Recent advances and perspectives in small-molecule TLR ligands and their modulators. *ACS Med. Chem. Lett.* **9**, 1156–1159 (2018).
18. Svajger, U. et al. Novel toll-like receptor 4 (TLR4) antagonists identified by structure- and ligand-based virtual screening. *Eur. J. Med. Chem.* **70**, 393–399 (2013).
19. Perez-Regidor, L., Zarioh, M., Ortega, L. & Martin-Santamaria, S. Virtual screening approaches towards the discovery of toll-like receptor modulators. *Int. J. Mol. Sci.* **17**, https://doi.org/10.3390/ijms17091508 (2016).
20. Zhang, B., Li, H., Yu, K. & Jin, Z. Molecular docking-based computational platform for high-throughput virtual screening. *CCF Trans. high. Perform. Comput.* **4**, 63–74 (2022).
21. Honegr, J. et al. Rational design of novel TLR4 ligands by in silico screening and their functional and structural characterization in vitro. *Eur. J. Med. Chem.* **146**, 38–46 (2018).

22. Pulendran, B., P, S. A. & O'Hagan, D. T. Emerging concepts in the science of vaccine adjuvants. *Nat. Rev. Drug. Discov.* **20**, 454–475 (2021).
23. Querec, T. et al. Yellow fever vaccine YF-17D activates multiple dendritic cell subsets via TLR2, 7, 8, and 9 to stimulate polyvalent immunity. *J. Exp. Med.* **203**, 413–424 (2006).
24. Koyama, S. et al. Differential role of TLR- and RLR-signaling in the immune responses to influenza A virus infection and vaccination. *J. Immunol.* **179**, 4711–4720 (2007).
25. Francica, J. R. et al. Innate transcriptional effects by adjuvants on the magnitude, quality, and durability of HIV envelope responses in NHPs. *Blood Adv.* **1**, 2329–2342 (2017).
26. Petitdemange, C. et al. Vaccine induction of antibodies and tissue-resident CD8 + T cells enhances protection against mucosal SHIV-infection in young macaques. *JCI insight* **4**, https://doi.org/10.1172/jci.insight.126047 (2019).
27. Didierlaurent, A. M. et al. AS04, an aluminum salt- and TLR4 agonist-based adjuvant system, induces a transient localized innate immune response leading to enhanced adaptive immunity. *J. Immunol.* **183**, 6186–6197 (2009).
28. Didierlaurent, A. M. et al. Adjuvant system AS01: helping to overcome the challenges of modern vaccines. *Expert Rev. Vaccines* **16**, 55–63 (2017).
29. Casella, C. R. & Mitchell, T. C. Putting endotoxin to work for us: monophosphoryl lipid A as a safe and effective vaccine adjuvant. *Cell. Mol. Life Sci.* **65**, 3231–3240 (2008).
30. Zhang, Y., Gaekwad, J., Wolfert, M. A. & Boons, G. J. Synthetic tetra-acylated derivatives of lipid A from Porphyromonas gingivalis are antagonists of human TLR4. *Org. Biomol. Chem.* **6**, 3371–3381 (2008).
31. Coler, R. N. et al. Development and characterization of synthetic glucopyranosyl lipid adjuvant system as a vaccine adjuvant. *PloS one* **6**, e16333 (2011).
32. Morefield, G. L., Hawkins, L. D., Ishizaka, S. T., Kissner, T. L. & Ulrich, R. G. Synthetic Toll-like receptor 4 agonist enhances vaccine efficacy in an experimental model of toxic shock syndrome. *Clin. Vaccine Immunol.* **14**, 1499–1504 (2007).
33. Park, B. S. et al. The structural basis of lipopolysaccharide recognition by the TLR4-MD-2 complex. *Nature* **458**, 1191–1195 (2009).
34. Ishizaka, S. T. & Hawkins, L. D. E6020: a synthetic Toll-like receptor 4 agonist as a vaccine adjuvant. *Expert Rev. Vaccines* **6**, 773–784 (2007).
35. Orr, M. T. et al. Adjuvant formulation structure and composition are critical for the development of an effective vaccine against tuberculosis. *J. Control. Rel.* **172**, 190–200 (2013).
36. Ding, D. et al. Self-adjuvanting protein vaccine conjugated with a novel synthetic TLR4 agonist on virus-like liposome induces potent immunity against SARS-CoV-2. *J. Medicinal Chem.* **66**, 1467–1483 (2023).
37. Rohokale, R., Guo, J. & Guo, Z. Monophosphoryl Lipid A-Rhamnose Conjugates as a New Class of Vaccine Adjuvants. *J. Med. Chem.* **67**, 7458–7469 (2024).
38. Wang, X., Smith, C. & Yin, H. Targeting Toll-like receptors with small molecule agents. *Chem. Soc. Rev.* **42**, 4859–4866 (2013).
39. Salunke, D. B. et al. Design and development of stable, water-soluble, human Toll-like receptor 2 specific monoacyl lipopeptides as candidate vaccine adjuvants. *J. Med. Chem.* **56**, 5885–5900 (2013).
40. Chan, M. et al. Identification of substituted pyrimido[5,4-b]indoles as selective Toll-like receptor 4 ligands. *J. Med. Chem.* **56**, 4206–4223 (2013).
41. Wang, Y. et al. TLR4/MD-2 activation by a synthetic agonist with no similarity to LPS. *Proc. Natl. Acad. Sci. USA* **113**, E884–E893 (2016).
42. Beesu, M., Salyer, A. C., Trautman, K. L., Hill, J. K. & David, S. A. Human Toll-like Receptor (TLR) 8-specific agonistic activity in substituted Pyrimidine-2,4-diamines. *J. Med. Chem.* **59**, 8082–8093 (2016).
43. Shukla, N. M. et al. Toward self-adjuvanting subunit vaccines: model peptide and protein antigens incorporating covalently bound toll-like receptor-7 agonistic imidazoquinolines. *Bioorg. Med. Chem. Lett.* **21**, 3232–3236 (2011).
44. Kokatla, H. P. et al. Toll-like receptor-8 agonistic activities in C2, C4, and C8 modified thiazolo[4,5-c]quinolines. *Org. Biomol. Chem.* **11**, 1179–1198 (2013).
45. Evans, J. T. et al. Synthetic Toll-like Receptors 7 and 8 agonists: structure-activity relationship in the Oxoadenine series. *ACS Omega* **4**, 15665–15677 (2019).
46. Kurimoto, A. et al. Synthesis and biological evaluation of 8-oxoadenine derivatives as toll-like receptor 7 agonists introducing the antedrug concept. *J. Med. Chem.* **53**, 2964–2972 (2010).
47. Dowling, D. J. Recent advances in the discovery and delivery of TLR7/8 agonists as vaccine adjuvants. *ImmunoHorizons* **2**, 185–197 (2018).
48. Fagan, V. et al. Synthesis, characterization and immunological evaluation of self-adjuvanting group a streptococcal vaccine candidates bearing various lipidic adjuvanting Moieties. *Chembiochem: Eur. J. Chem. Biol.* **18**, 545–553 (2017).
49. Chan, A. L., Leung, H. W., Lu, C. L. & Lin, S. J. Cost-effectiveness of trastuzumab as adjuvant therapy for early breast cancer: a systematic review. *Ann. Pharmacother.* **43**, 296–303 (2009).
50. Perez-Regidor, L. et al. Small molecules as toll-like Receptor 4 modulators drug and in-house computational repurposing. *Biomedicines* **10**, https://doi.org/10.3390/biomedicines10092326 (2022).
51. Paier, C. R. K. et al. Natural products as new antimitotic compounds for anticancer drug development. *Clinics* **73**, e813s (2018).
52. Marshall, J. D. et al. A Novel class of small molecule agonists with preference for human over mouse TLR4 activation. *PlLoS One* **11**, e0164632 (2016).
53. Fakhar, Z., Hejazi, L., Tabatabai, S. A. & Munro, O. Q. Discovery of novel heterocyclic amide-based inhibitors: an integrative in-silico approach to targeting soluble epoxide hydrolase. *J. Biomol. Struct. Dyn.* **40**, 7114–7128 (2022).
54. Ferreira, L. L. G. & Andricopulo, A. D. ADMET modeling approaches in drug discovery. *Drug. Discov. Today* **24**, 1157–1165 (2019).
55. Dolezal, R. et al. Ligand-based 3D QSAR analysis of reactivation potency of mono- and bis-pyridinium aldoximes toward VX-inhibited rat acetylcholinesterase. *J. Mol. Graph. Model.* **56**, 113–129 (2015).
56. Wang, X. et al. Docking and CoMSIA studies on steroids and non-steroidal chemicals as androgen receptor ligands. *Ecotoxicol. Environ. Saf.* **89**, 143–149 (2013).
57. Vaure, C. & Liu, Y. A comparative review of toll-like receptor 4 expression and functionality in different animal species. *Front. Immunol.* **5**, 316 (2014).
58. Xu, S. et al. Impact of adjuvants on the biophysical and functional characteristics of HIV vaccine-elicited antibodies in humans. *NPJ Vaccines* **7**, 90 (2022).
59. Murgueitio, M. S. et al. Enhanced immunostimulatory activity of in silico discovered agonists of Toll-like receptor 2 (TLR2). *Biochim. Biophys. acta. Gen. Subj.* **1861**, 2680–2689 (2017).
60. Triantafilou, M. & Triantafilou, K. The dynamics of LPS recognition: complex orchestration of multiple receptors. *J. Endotoxin Res.* **11**, 5–11 (2005).
61. Wang, Y. et al. MD-2 as the target of a novel small molecule, L6H21, in the attenuation of LPS-induced inflammatory response and sepsis. *Br. J. Pharmacol.* **172**, 4391–4405 (2015).
62. Kawasaki, K., Nogawa, H. & Nishijima, M. Identification of mouse MD-2 residues important for forming the cell surface TLR4-MD-2 complex recognized by anti-TLR4-MD-2 antibodies, and for conferring LPS and taxol responsiveness on mouse TLR4 by alanine-scanning mutagenesis. *J. Immunol.* **170**, 413–420 (2003).

63. Michaeli, A. et al. Computationally designed bispecific MD2/CD14 binding peptides show TLR4 agonist activity. *J. Immunol.* **201**, 3383–3391 (2018).
64. Perrin-Cocon, L. et al. TLR4 antagonist FP7 inhibits LPS-induced cytokine production and glycolytic reprogramming in dendritic cells, and protects mice from lethal influenza infection. *Sci. Rep.* **7**, 40791 (2017).
65. Fan, H. & Cook, J. A. Molecular mechanisms of endotoxin tolerance. *J. Endotoxin Res.* **10**, 71–84 (2004).
66. Medzhitov, R. & Janeway, C. Jr. Innate immune recognition: mechanisms and pathways. *Immunol. Rev.* **173**, 89–97 (2000).
67. Zughaier, S. M., Shafer, W. M. & Stephens, D. S. Antimicrobial peptides and endotoxin inhibit cytokine and nitric oxide release but amplify respiratory burst response in human and murine macrophages. *Cell. Microbiol.* **7**, 1251–1262 (2005).
68. Shen, H., Tesar, B. M., Walker, W. E. & Goldstein, D. R. Dual signaling of MyD88 and TRIF is critical for maximal TLR4-induced dendritic cell maturation. *J. Immunol.* **181**, 1849–1858 (2008).
69. Romerio, A. & Peri, F. Increasing the chemical variety of small-molecule-based TLR4 modulators: an overview. *Front. Immunol.* **11**, 1210 (2020).
70. Cekic, C. et al. Selective activation of the p38 MAPK pathway by synthetic monophosphoryl lipid A. *J. Biol. Chem.* **284**, 31982–31991 (2009).
71. Sato-Kaneko, F. et al. A novel synthetic dual agonistic Liposomal TLR4/7 adjuvant promotes broad immune responses in an influenza vaccine with minimal reactogenicity. *Front. Immunol.* **11**, 1207 (2020).
72. Facchini, F. A. et al. Synthetic Glycolipids as molecular vaccine adjuvants: mechanism of action in human cells and in vivo activity. *J. Med. Chem.* **64**, 12261–12272 (2021).
73. Saito, T. et al. Small molecule potentiator of adjuvant activity enhancing survival to influenza viral challenge. *Front. Immunol.* **12**, 701445 (2021).
74. Stoute, J. A. et al. A preliminary evaluation of a recombinant circumsporozoite protein vaccine against Plasmodium falciparum malaria. RTS,S Malaria Vaccine Evaluation Group. *New. Engl. J. Med.* **336**, 86–91 (1997).
75. Diez-Domingo, J. et al. Immunogenicity and Safety of H5N1 A/Vietnam/1194/2004 (Clade 1) AS03-adjuvanted prepandemic candidate influenza vaccines in children aged 3 to 9 years: a phase ii, randomized, open, controlled study. *Pediatr. Infect. Dis. J.* **29**, e35–e46 (2010).
76. Giannini, S. L. et al. Enhanced humoral and memory B cellular immunity using HPV16/18 L1 VLP vaccine formulated with the MPL/aluminium salt combination (AS04) compared to aluminium salt only. *Vaccine* **24**, 5937–5949 (2006).
77. Del Giudice, G., Rappuoli, R. & Didierlaurent, A. M. Correlates of adjuvanticity: A review on adjuvants in licensed vaccines. *Semin. Immunol.* **39**, 14–21 (2018).
78. Petrovsky, N. Comparative safety of vaccine adjuvants: a summary of current evidence and future needs. *Drug. Saf.* **38**, 1059–1074 (2015).
79. Lipschitz, D. A., Cook, J. D. & Finch, C. A. A clinical evaluation of serum ferritin as an index of iron stores. *New. Engl. J. Med.* **290**, 1213–1216 (1974).
80. Haschka, D., Hoffmann, A. & Weiss, G. Iron in immune cell function and host defense. *Semin. Cell. Dev. Biol.* **115**, 27–36 (2021).
81. Davis, J. S., Ferreira, D., Paige, E., Gedye, C. & Boyle, M. Infectious complications of biological and small molecule targeted immunomodulatory therapies. *Clin. Microbiol. Rev.* **33**, https://doi.org/10.1128/CMR.00035-19 (2020).
82. Tarantino, G., Scalera, A. & Finelli, C. Liver-spleen axis: intersection between immunity, infections and metabolism. *World J. Gastroenterol.* **19**, 3534–3542 (2013).
83. Boess, F. G. et al. Analysis of the ligand binding site of the 5-HT3 receptor using site directed mutagenesis: importance of glutamate 106. *Neuropharmacology* **36**, 637–647 (1997).
84. Aliebrahimi, S., Montasser Kouhsari, S., Ostad, S. N., Arab, S. S. & Karami, L. Identification of phytochemicals targeting c-Met kinase domain using consensus docking and molecular dynamics simulation studies. *Cell. Biochem. Biophys.* **76**, 135–145 (2018).
85. Forli, S. et al. Computational protein-ligand docking and virtual drug screening with the AutoDock suite. *Nat. Protoc.* **11**, 905–919 (2016).
86. Honegr, J. et al. Rational design of a new class of toll-like Receptor 4 (TLR4) Tryptamine related agonists by means of the structure- and ligand-based virtual screening for vaccine adjuvant discovery. *Molecules* **23**, https://doi.org/10.3390/molecules23010102 (2018).
87. Lipinski, C. A. Lead- and drug-like compounds: the rule-of-five revolution. *Drug. Discov. Today Technol.* **1**, 337–341 (2004).
88. Wienken, C. J., Baaske, P., Rothbauer, U., Braun, D. & Duhr, S. Protein-binding assays in biological liquids using microscale thermophoresis. *Nat. Commun.* **1**, 100 (2010).
89. Faisal, S. M. et al. Immunostimulatory and antigen delivery properties of liposomes made up of total polar lipids from non-pathogenic bacteria leads to efficient induction of both innate and adaptive immune responses. *Vaccine* **29**, 2381–2391 (2011).
90. van de Loosdrecht, A. A., Beelen, R. H., Ossenkoppele, G. J., Broekhoven, M. G. & Langenhuijsen, M. M. A tetrazolium-based colorimetric MTT assay to quantitate human monocyte mediated cytotoxicity against leukemic cells from cell lines and patients with acute myeloid leukemia. *J. Immunol. Methods* **174**, 311–320 (1994).
91. Varma, V. P., Kadivella, M., Kumar, A., Kavela, S. & Faisal, S. M. LigA formulated in AS04 or Montanide ISA720VG induced superior immune response compared to alum, which correlated to protective efficacy in a Hamster model of leptospirosis. *Front. Immunol.* **13**, 985802 (2022).
92. Patra, C. R. et al. In vivo toxicity studies of europium hydroxide nanorods in mice. *Toxicol. Appl. Pharmacol.* **240**, 88–98 (2009).

Acknowledgements

This work was supported by the Indo-US grant- BT/PR34488/MED/15/221/2022(SP094) on developing potent Vaccine Adjuvants. The project was funded to SMF by the Department of Biotechnology under the Ministry of Science and Technology, Government of India. Financial support from the NIAB core funds (C0023) is duly acknowledged. The authors would like to thank the Director, NIAB, for providing the necessary infrastructural facility and support for the execution of the above study. We thank the staff of the Animal Resource and Experimental Facility for assistance in the animal experiments. MK and JCP were supported by UGC and CSIR fellowships and registered for the Ph.D. programme at RCB, Faridabad. The funders had no role in study design, data collection and analysis, decision to publish, or preparation of the manuscript.

Author contributions

Conceptualization: S.M.F. Methodology: M.K., V.P.V., J.C.P., S.K. Investigation and formal analysis: M.K., J.C.P., S.M.F. In silico analysis: M.K. and S.A. Writing—original draft preparation: M.K., J.C.P. Review and editing: S.M.F. Resources: S.M.F. Study supervision: S.M.F. Funding acquisition: S.M.F. Final approval: all authors.

Competing interests

The authors declare no competing financial interests. A patent has been granted for NSF-951 and its formulation AF007, titled "*Synthetic NSF-951 Agonist Compound and Preparation Thereof, Antigen-Alum-Synthetic NSF-951 Immuno-Formulation*" (Patent No. 569943, dated 21 August 2025).

Additional information

Supplementary information The online version contains supplementary material available at https://doi.org/10.1038/s42003-025-08582-y.

Correspondence and requests for materials should be addressed to Syed M. Faisal.

Peer review information *Communications Biology* thanks the anonymous reviewers for their contribution to the peer review of this work. Primary Handling Editors: Xiaoling Xu and Laura Rodríguez Pérez. A peer review file is available.